Aw 7/28/52

NACA TN 2729

NATIONAL ADVISORY COMMITTEE FOR AERONAUTICS

TECHNICAL NOTE 2729

AN ANALYSIS OF SUPERSONIC FLOW IN THE REGION OF THE LEADING EDGE OF CURVED AIRFOILS, INCLUDING CHARTS FOR DETERMINING SURFACE-PRESSURE GRADIENT AND SHOCK-WAVE CURVATURE

By Samuel Kraus

Ames Aeronautical Laboratory
Moffett Field, Calif.

DISTRIBUTION STATEMENT A
Approved for Public Release
Distribution Unlimited

Washington
June 1952

Reproduced From
Best Available Copy

20000505 087

M00-08-2221

1X

NATIONAL ADVISORY COMMITTEE FOR AERONAUTICS

TECHNICAL NOTE 2729

AN ANALYSIS OF SUPERSONIC FLOW IN THE REGION OF THE LEADING EDGE OF CURVED AIRFOILS, INCLUDING CHARTS FOR DETERMINING SURFACE-PRESSURE GRADIENT AND SHOCK-WAVE CURVATURE

By Samuel Kraus

SUMMARY

Inviscid flow in the region of the leading edge of curved airfoils with attached shock waves is investigated. Tables and charts are presented for determining the surface-pressure gradient and the shock-wave curvature in supersonic flow of an ideal diatomic gas. The results cover a range of Mach numbers from 1.5 to infinity and deflection angles from zero up to those approaching shock detachment. Calculations of surface-pressure gradient and shock-wave curvature are also made for curved airfoils in supersonic flow of a calorically imperfect, diatomic gas. These calculations are quantitatively applicable in cases where the air temperatures, downstream of the shock wave, do not exceed about 5000° Rankine.

When flow conditions approach those at which shock waves detach from airfoils, the surface-pressure gradient and shock-wave curvature vary widely from the values predicted by a generalized shock-expansion method. Otherwise, the use of the shock-expansion method introduces only small errors, particularly in the case of ideal gas flows. The effect of caloric imperfections in air is to increase these errors.

An approximate procedure for determining the flow field a short distance downstream of the leading edge is also presented.

INTRODUCTION

Flow in the region of the leading edge of an airfoil with attached shock wave has been studied by numerous investigators, including Crocco (reference 1), and more recently Munk and Prim (reference 2), Schaefer (reference 3), and Thomas (reference 4). With the assumptions that the flow is steady, two-dimensional, and inviscid, and that air behaves as an

ideal (diatomic) gas, it has been found that effects on the flow of interaction between the shock wave emanating from the leading edge and other disturbances emanating from the surface can be calculated. It is to be expected, therefore, that within the limitations of these assumptions, such parameters as surface-pressure gradient and shock-wave curvature at the leading edge of an airfoil can be accurately predicted. The first purpose of the present report is to present values of these parameters for a wide range of Mach numbers and flow deflection angles, thereby supplementing and extending the results presented in reference 2.

Supersonic flow about airfoils was investigated more generally by Eggers and Syvertson (reference 5) and it was found that caloric imperfections in air influence the flow appreciably at higher Mach numbers where the temperatures of the disturbed air are well above ambient temperatures. They used a generalized method of characteristics to take into account these imperfections at temperatures up to about 5000° Rankine. It was further shown that the shock-expansion method, generalized to include major effects of interaction between shock waves and disturbances incident thereon and to account for effects of caloric imperfections, should predict the flow field about an airfoil with reasonable accuracy. The advantage of this method over the method of characteristics is, of course, its relative simplicity.

Flow in the region of the leading edge of an airfoil was not considered in detail, however, in reference 5. An additional objective of the present paper is, then, to determine effects of caloric imperfections on flow in this region, using a method analogous to that of Munk and Prim for ideal gas flows, particular attention being given to surface-pressure gradient and shock-wave curvature at the leading edge. Predictions of these quantities by the generalized shock-expansion method are also presented for both ideal and calorically imperfect gas flows.

Since it is useful to know the flow conditions a short distance downstream of the leading edge (e.g., to start characteristics solutions for flow about airfoils), an approximate method of determining this flow field is also discussed. This method depends on a knowledge of the surface-pressure gradient and shock-wave curvature at the leading edge.

SYMBOLS

C_1, C_2 characteristic coordinates, feet

K curvature, feet^{-1}

M Mach number (ratio of local velocity to local speed of sound)

P ratio of static pressure downstream of the shock wave to free-stream static pressure

T absolute temperature, degrees Rankine

W distance measured from leading edge along airfoil surface, feet

x, y rectangular coordinates, feet

α Mach angle $\left(\text{arc sin } \frac{1}{M}\right)$, degrees

β angle between shock wave and flow direction just downstream of the shock wave, degrees

γ ratio of specific heat at constant pressure to specific heat at constant volume

δ angle between flow direction just downstream of the shock wave and flow direction of the free stream, degrees

θ molecular vibrational energy constant, degrees Rankine (5500° R for air)

κ ratio of the shock-wave curvature to that given by the shock-expansion method

ρ ratio of density just downstream of the shock wave to the free-stream density

σ angle between flow direction of free stream and shock wave, degrees

ψ ratio of surface-pressure gradient to that given by the shock-expansion method

Subscripts

o free-stream conditions

i ideal gas quantities

N conditions at the leading edge immediately downstream of the shock wave

s conditions along the shock wave

w conditions along the airfoil surface

ANALYSIS OF FLOW IN THE REGION OF THE LEADING EDGE

Calculation of Surface-Pressure Gradient and Shock-Wave Curvature

A curved two-dimensional airfoil surface creates pressure disturbances which alter the inclination of an attached leading-edge shock wave. Figure 1 illustrates the geometry of this phenomenon for a convex airfoil. The pressure disturbances (expansion waves for a convex airfoil) travel along first-family Mach lines C_1 and interact with the oblique shock wave. In addition to changing the inclination of the shock wave, this interaction produces another system of disturbances which travel along second-family Mach lines C_2 from the shock wave to the body.

Method of characteristics.- An exact solution for the surface-pressure gradient and shock-wave curvature at the leading edge may be determined by the method of characteristics in the following manner. It is clear, referring to figure 1, that the difference in flow angle between points A and C given by the compatibility equations (see reference 2)

$$\left(\frac{d\delta}{dP}\right)_{C_1} = -\frac{\sin 2\alpha}{2\gamma P} \tag{1}$$

and

$$\left(\frac{d\delta}{dP}\right)_{C_2} = \frac{\sin 2\alpha}{2\gamma P} \tag{2}$$

along the path ABC must equal that determined by the airfoil surface from A to C. Also, the difference in pressure between points B and D given by these compatibility equations along the path BCD must equal that determined by the change in shock-wave inclination between B and D. In reference 2, these conditions were employed at the leading edge to obtain equations, in a simple parametric form, for determining the surface-pressure gradients and the shock-wave curvatures.

These equations can be written in the form

$$\frac{1}{K_W}\frac{dP}{dW} = \frac{Z+1}{(Z-1)\left(\frac{d\delta}{dP}\right)_{C_2}} \tag{3}$$

for the surface-pressure gradient, and

$$\frac{K_s}{K_w} = \frac{Z \sin(\alpha - \sigma + \delta) - \sin(\alpha + \sigma - \delta)}{(Z-1) \sin \alpha \left(\frac{d\delta}{d\sigma}\right)_s} \tag{4}$$

for the shock-wave curvature, where

$$Z = \frac{\partial P/\partial C_2}{\partial P/\partial C_1} = \left[\frac{(dP/d\delta)_s \, (d\delta/dP)_{C_2} + 1}{(dP/d\delta)_s \, (d\delta/dP)_{C_2} - 1}\right] \left[\frac{\sin(\alpha + \sigma - \delta)}{\sin(\alpha - \sigma + \delta)}\right] \tag{5}$$

A procedure for evaluating equations (3) and (4) for a calorically imperfect, diatomic gas, as well as for an ideal gas, is presented in the appendix of this report. The values of surface-pressure gradient and shock-wave curvature at the leading edge determined using these equations are exact for two-dimensional, steady, inviscid flows.

Two applications of these equations will be considered: First, the accuracy of approximate methods of calculating the flow field about a curved airfoil can be evaluated at the leading edge by comparing the values of surface-pressure gradient and shock-wave curvature predicted by these approximate methods to the values obtained using equations (3) and (4). Second, the pressure gradient and shock-wave curvature can be used to determine the approximate flow field, between the body and the shock wave, a short distance downstream of the leading edge and thereby obtain the initial points of a characteristics solution.

Shock-expansion method.- An approximate solution for the surface-pressure gradient and shock-wave curvature may be obtained using the shock-expansion method. Eggers and Syvertson (reference 5), in their general discussion of the entire flow field about airfoils, found that disturbances incident on an oblique shock wave were almost entirely consumed in changing the shock-wave inclination, and that the reflected disturbances were weak enough, in most cases, to be neglected. Thus, as a first approximation, the deflection angle and pressure, but not necessarily the Mach number and entropy, can be considered constant along first-family Mach lines. The use of this assumption leads to a generalized shock-expansion method for calculating the entire flow field about an airfoil. The application of this approximate method to the analysis of flow in the region of the leading edge is now considered.

If the disturbances reflected from the shock wave can be neglected,

$$\frac{\partial P}{\partial C_1} << \frac{\partial P}{\partial C_2} \tag{6}$$

Hence, from equation (5), Z must be large compared to unity. If this approximation is made, the expression for the surface-pressure gradient (equation (3)) reduces to

$$\frac{1}{K_W}\frac{dP}{dW} = \frac{1}{(d\delta/dP)_{C_2}} \tag{7}$$

Similarly, the expression for the shock-wave curvature (equation (4)) reduces to

$$\frac{K_S}{K_W} = \frac{\sin(\alpha - \sigma + \delta)}{\left(\frac{d\delta}{d\sigma}\right)_S \sin\alpha} \tag{8}$$

It should be realized that the flow field is determined by the basic flow equations in conjunction with the shock wave and airfoil surface as boundary conditions. Thus, the additional requirement for this shock-expansion method of zero pressure gradient along first-family Mach lines means that one of the flow relations cannot be satisfied exactly (i.e., the flow field is overdetermined). Equations (7) and (8) satisfy the shock relations and the airfoil surface as boundary conditions; however, the compatibility equations are only approximately satisfied.

The error in surface-pressure gradient associated with neglecting the reflected disturbances might be expected to be largest in the region of the leading edge of a curved airfoil due to the close proximity of the shock wave and the surface. The magnitude of the error in this region may be deduced, of course, from the ratios of values of surface-pressure gradient and shock-wave curvature given by the characteristics method to those given by the shock-expansion method. The surface-pressure-gradient ratio and shock-wave-curvature ratio can be written (using equations (3) and (7))

$$\psi = \frac{Z + 1}{Z - 1} \tag{9}$$

and (using equations (4) and (8))

$$\kappa = \frac{Z \sin(\alpha - \sigma + \delta) - \sin(\alpha + \sigma - \delta)}{(Z - 1)\sin(\alpha - \sigma + \delta)} \tag{10}$$

respectively. A procedure for evaluating equations (9) and (10) for flow of a calorically imperfect gas, as well as for an ideal gas, is presented in the appendix of this report. (The application of equation (9) for ideal gas flow has already been given in reference 2.)

Calculation of the Flow Field a Short Distance Downstream of the Leading Edge

A knowledge of the values of flow parameters along a line from the body to the shock wave is useful in starting characteristics or shock-expansion solutions for the entire flow field. A method is now presented for approximating these parameters along a first-family Mach line a short distance downstream of the leading edge. In the region of the leading edge, the airfoil, the shock wave, and a first-family Mach line are approximated by circular arcs, as shown in figure 2. The equations of the airfoil surface and the shock wave can then be written (knowing the slope and curvature at the leading edge)

$$y_w = -\frac{\cos \delta_N}{K_{w_N}} + \frac{\sqrt{1 - (K_{w_N} x_w - \sin \delta_N)^2}}{K_{w_N}} \tag{11}$$

and

$$y_s = -\frac{\cos \sigma_N}{K_{s_N}} + \frac{\sqrt{1 - (K_{s_N} x_s - \sin \sigma_N)^2}}{K_{s_N}} \tag{12}$$

respectively. If it is assumed that the pressure gradient is constant along the airfoil surface for a short distance downstream of the leading edge, the pressure distribution and thus all other flow conditions at the surface are known since the flow conditions at the leading edge are known (see previous analysis). Since the shock wave is approximated by a circular arc, the flow conditions just downstream of the shock wave are also known. Thus, the flow parameters, and consequently the slopes of a first-family Mach line, will be known at its intersections with the body and the shock wave. The problem, then, is to determine the curvature, and thus the equation of this Mach line. The following analysis is devoted to this matter.

To the accuracy of the present analysis, the flow angle δ and the Mach angle α vary linearly with distance along the Mach line. Thus (see fig. 2)

$$\frac{y_B - y_A}{x_B - x_A} = \tan \frac{1}{2} \left[(\alpha_w + \delta_w)_A + (\alpha_s + \delta_s)_B \right] \tag{13}$$

where the local flow angle and local Mach angle at the airfoil surface can be written (as a first approximation)

$$\delta_A \cong \delta_N + \left(\frac{d\delta}{dW}\right)_N \left(\frac{dW}{dx}\right)_N x_A \cong \delta_N + K_{w_N} x_A \sec \delta_N \tag{14}$$

and

$$\alpha_A \cong \alpha_N + \left(\frac{d\alpha}{dP}\right)_{w_N} \left(\frac{1}{K_w} \frac{dP}{dW}\right)_N K_{w_N} x_A \sec \delta_N \tag{15}$$

respectively.

Similarly, at the shock wave,

$$\delta_B \cong \delta_N + \left(\frac{d\delta}{d\sigma}\right)_{s_N} K_{s_N} x_B \sec \sigma_N \tag{16}$$

and

$$\alpha_B \cong \alpha_N + \left(\frac{d\alpha}{d\sigma}\right)_{s_N} K_{s_N} x_B \sec \sigma_N \tag{17}$$

It is possible to determine $\left(\frac{d\alpha}{d\sigma}\right)_{s_N}$, $\left(\frac{d\delta}{d\sigma}\right)_{s_N}$, and $\left(\frac{d\alpha}{dP}\right)_{w_N}$ for imperfect gas flow as well as for ideal gas flow. Thus, an implicit relation between x_s and x_w can be found from equations (11) through (17).

The equation of the circular arc approximating the first-family Mach line may be written, for any initial x_w (knowing the slopes at the intersection of this line with the shock wave and the body)

$$y_{C_1} = -\frac{\cos \delta_N}{K_{w_N}} + \frac{\sqrt{1 - (K_{w_N} x_w - \sin \delta_N)^2}}{K_{w_N}} - \frac{\cos (\alpha_w + \delta_w)}{K_{C_1}} + \frac{\sqrt{1 - \left[K_{C_1} x_{C_1} - K_{C_1} x_w - \sin (\alpha_w + \delta_w)\right]^2}}{K_{C_1}} \tag{18}$$

At point B, the intersection of the shock wave and the first-family Mach line, equation (18) may be solved for K_{C_1}, using the implicit relation between x_s and x_w. Substituting this value of K_{C_1} into equation (18), an equation relating y_{C_1} and x_{C_1} along the first-family Mach line can be found for every value of x_w.

The pressure and flow angle at A and B and the changes in pressure and flow angle from A to B may be determined. The change in pressure with change in flow angle should agree (to the desired degree of accuracy) with that calculated using the basic compatibility relation, namely,

$$\left.\frac{\Delta P}{\Delta \delta}\right|_A^B \cong -\frac{\gamma(P_A + P_B)}{\sin(\alpha_A + \alpha_B)}$$

Any significant difference should be diminished by choosing point A closer to the leading edge.

The angles δ and α are known at each point along this first-family Mach line, and the pressure variation may be determined using the characteristics compatibility equation (equation (1)). Hence the entropy variation can also be determined. Therefore, all necessary flow parameters are defined along this line, rendering it a good starting line for a characteristics solution for the entire flow field.

DISCUSSION

Ideal Gas Flows

Surface-pressure gradient.- The results of the calculations (using equation (A4) of the appendix) of surface-pressure gradient are presented in table I and figures 3 and 4. The values presented in table I are for a range of Mach numbers from 1.5 to ∞ and for leading-edge deflection angles from 0° to 45°. Where no value appears in the table, the flow behind the shock wave is subsonic. Additional calculations, not presented in the table, were made to permit the accurate plotting of curves to the point where the flow behind the shock wave attains sonic velocity.[1]

[1]Charts were also presented for surface-pressure gradient, surface-pressure-gradient ratio, and shock-wave curvature for ideal gas flows in reference 2; however, the results given in the present report are somewhat more extensive.

Surface-pressure-gradient ratio.- The results of the calculations of surface-pressure-gradient ratio (equation (A6)) are presented in table II and figures 5 and 6 in a manner similar to the presentation of the surface-pressure gradient. From these results, it is seen that, except near detachment, the surface-pressure-gradient ratio varies between approximately 0.88 and 1.12 for all Mach numbers including ∞. Below a Mach number of 4 the ratio varies only from 0.98 to 1.02, except near detachment. Therefore, little error will result from the use of the shock-expansion method for the surface-pressure gradient at the leading edge of airfoils for Mach numbers less than 4. Near detachment, for Mach numbers greater than approximately 2, the surface-pressure-gradient ratio attains a very large range of values. The maximum value of the ratio increases with Mach number. The use of the surface-pressure gradient at the leading edge as given by the shock-expansion method would result in appreciable error near detachment conditions.

It should be noted that, for the particular case of infinite free-stream Mach number and zero deflection angle, the pressure-gradient ratio ψ is double-valued. From equation (A6), it is apparent that ψ is 1 for zero deflection. Yet, at infinite free-stream Mach number, ψ approaches 0.882[2] as the deflection angle approaches zero.

The flow along the surface is isentropic. Hence, it can be shown that ψ, the ratio of surface-pressure gradient to that given by the generalized shock-expansion method, is also the velocity-gradient ratio, the Mach number gradient ratio, the Mach angle gradient ratio, the density-gradient ratio, and the temperature-gradient ratio. Any of these gradients may be found, then, by calculating the gradient using the shock-expansion method and applying the appropriate value of ψ. This property of the ratio ψ makes it useful in the application of the method of characteristics with any of the coordinate systems commonly employed in the compatibility equations.

Shock-wave curvature.- The results of the calculations of shock-wave curvature (equation (A5)) are presented in table III and figures 7 and 8. It is clear from equation (A5) that K_s/K_w is zero for zero deflection angle. However, when the free-stream Mach number is infinite, K_s/K_w approaches 0.800[3] as the deflection angle approaches zero. Thus, K_s/K_w is double-valued at $M = \infty$, $\delta = 0$.

---

[2]The precise value of ψ for this limit is $\frac{3}{2\gamma - 1}\sqrt{\frac{\gamma(\gamma - 1)}{2}}$.

[3]The limiting value of K_s/K_w is $\frac{(\gamma + 1)^2}{4(2\gamma - 1)}$.

Shock-wave-curvature ratio.- The shock-wave-curvature ratio for various free-stream Mach numbers and deflection angles has been calculated by means of equations (8) and (A5). The results of these calculations are presented in table IV and figures 9 and 10. It is interesting to note that the curves in figure 9 are similar to the reciprocals of the curves shown in figure 5. Indeed, this conclusion can be deduced by comparing equations (9) and (10). Except near detachment, the curvature ratio varies from 0.92 to 1.08 for all Mach numbers including ∞. Thus, only moderate errors would result from using the value of shock-wave curvature given by the shock-expansion method for all flow conditions except near detachment. For zero deflection angle, it is apparent from equation (10) that κ must be 1. However, for infinite free-stream Mach number, κ approaches 1.072[4] as the deflection angle approaches zero. Thus κ is also double-valued.

Calorically Imperfect Gas Flows

The temperature ratio across an oblique shock wave increases with increasing Mach number and leading-edge slope, as shown in figure 11. As the temperature behind the shock wave increases, the behavior of the air diverges from that of an ideal gas. Below 800° Rankine, the divergence is not significant, and the equations for ideal gas flow can be applied with only minute errors resulting.

Above 800° Rankine, the energy of the vibrational degrees of freedom of the gas molecules is appreciable and becomes greater with increasing temperature. As a result, the ratio of specific heats varies with temperature, as discussed by Eggers in reference 6.

As mentioned previously, equations were developed in reference 5 permitting the calculation of the flow of a diatomic, calorically imperfect gas about two-dimensional airfoils. These equations apply for temperatures up to the order of 5000° Rankine and form the basis for the extension of the solution for surface-pressure gradient, surface-pressure-gradient ratio, shock-wave curvature, and shock-wave-curvature ratio to the case of calorically imperfect gases. For a free-stream temperature of 500° Rankine, the shaded area between lines of constant temperature ratio of 1.5 and 10, in figure 11, represents the approximate range of conditions for which the method developed in this report for the flow of a diatomic, calorically imperfect gas would apply. The range shown in figure 11 is only approximate, since it was calculated using ideal gas-flow equations.

---

[4]The exact limiting value of κ is $\dfrac{\gamma + 1}{2(2\gamma - 1)\left(1 - \sqrt{\dfrac{\gamma - 1}{2\gamma}}\right)}$.

The excitation of the vibrational degrees of freedom of the gas molecules requires a finite number of collisions, causing the well-known heat-capacity lag discussed by Bethe and Teller in reference 7. The flow distance (i.e., along the streamline) required to establish equilibrium conditions is usually small in dense air and will be considered infinitesimal in this report.[5]

Since the free-stream static temperature is an additional parameter in calculations of flow of imperfect gases, only a limited number of calculations of $(1/K_W)(dP/dW)$, ψ, K_S/K_W, and κ were made. The purpose of these calculations is to compare the variations of these quantities with the values as given by the ideal-gas-flow computations. The calculations followed the procedure described in the appendix. A free-stream static temperature of 500° Rankine was used. The results of these calculations are presented in table V for various Mach numbers and leading-edge deflection angles.

The surface-pressure gradients for an ideal gas and for a calorically imperfect, diatomic gas are compared in figure 12. In all cases calculated, the gradient is smaller for the imperfect gas and diverges gradually, with increasing free-stream Mach number and deflection angle, from the value of the gradient for an ideal gas. This divergence is consistent with the increasing effects of the caloric imperfections due to the increasing temperature behind the shock wave.

The surface-pressure-gradient ratio for the imperfect gas is compared in figure 13 with the ratio for an ideal gas. The angle β between the shock wave and the leading edge of the airfoil is smaller for imperfect gas flows than for ideal gas flows, and shock-wave expansion-wave interaction effects are increased. As a result, the surface-pressure-gradient ratio is smaller for imperfect gas flows than for ideal gas flows. This difference in the angle β is a function of the temperature behind the shock wave. Thus, the surface-pressure-gradient ratio for imperfect gas flows diverges from the ratio for ideal gas flows with increasing Mach number and deflection angle.

A divergence with Mach number and deflection angle is also apparent in figure 14 in which is compared the shock-wave curvature for an ideal gas and a calorically imperfect, diatomic gas. This divergence is compatible with the change in surface-pressure gradient due to the caloric imperfections of the gas.

---

[5] The dissociation of air at temperatures greater than about 5000° Rankine is also discussed in reference 7. This phenomenon is not considered in the present report.

The shock-wave-curvature ratio for a calorically imperfect, diatomic gas and this ratio for an ideal gas are shown in figure 15. Again it is seen that the effect of caloric imperfection is to increase the effects of shock-wave expansion-wave interaction.

CONCLUDING REMARKS

The supersonic flow field in the region of the leading edge of curved two-dimensional airfoils has been investigated.

A set of tables and charts has been presented giving the surface-pressure gradient and shock-wave curvature at the leading edge for an ideal gas for a large range of free-stream Mach numbers and leading-edge deflection angles. Previously derived equations for surface-pressure gradient and shock-wave curvature have been extended to permit the determination of these quantities for flow of a calorically imperfect, diatomic gas. Both the previously derived equations and the extended equations have been modified so that the shock-wave curvature and surface-pressure gradient are consistent with the assumptions of a generalized shock-expansion method. Values of surface-pressure gradient and shock-wave curvature have been compared with the values given by the modified equations. It has been shown that, except near conditions at which the shock wave detaches from the airfoil, only moderate errors would result from using the values given by shock-expansion equations for flow of an ideal gas. It has also been shown that caloric imperfections of air increase the error.

An approximate procedure has been presented for determining the flow field a short distance downstream of the leading edge. This procedure depends on a knowledge of the surface-pressure gradient and shock-wave curvature at the leading edge.

Ames Aeronautical Laboratory,
National Advisory Committee for Aeronautics,
Moffett Field, Calif., Mar. 31, 1952.

APPENDIX

EVALUATION OF $(1/K_w)(dP/dW)$, K_s/K_w, ψ, and κ

For an ideal gas, the Mach number, Mach angle, shock-wave angle, and pressure ratio can be calculated at the leading edge using the standard Rankine-Hugoniot shock relations and utilizing the free-stream Mach number and leading-edge deflection angle. Hence $(d\delta/dP)_{C_2}$ can be determined from equation (2) of the analysis. With these flow parameters known, the only terms still to be determined in equations (3), (4), (5), (9), and (10) are $(dP/d\delta)_s$ and $(d\delta/d\sigma)_s$.

Now (see reference 2)

$$\left(\frac{dP}{d\delta}\right)_s = \frac{(dP/d\sigma)_s}{(d\delta/d\sigma)_s} \tag{A1}$$

where

$$\left(\frac{dP}{d\sigma}\right)_s = \frac{2\,\gamma\,M_o^{\,2}\sin 2\,\sigma}{\gamma + 1} \tag{A2}$$

and

$$\left(\frac{d\delta}{d\sigma}\right)_s = 1 - \frac{\dfrac{\dfrac{\gamma+1}{2(\gamma-1)}\left(M_o^{\,2}\sin 2\,\sigma\right)^2 - \left(\dfrac{2}{\gamma-1} + M_o^{\,2}\sin^2\sigma\right)\left(\dfrac{\gamma+1}{\gamma-1}M_o^{\,2}\cos 2\,\sigma\right)}{\left[\dfrac{\gamma+1}{2(\gamma-1)}M_o^{\,2}\sin 2\,\sigma\right]^2}}{1 + \left[\dfrac{\dfrac{2}{\gamma-1} + M_o^{\,2}\sin^2\sigma}{\dfrac{\gamma+1}{2(\gamma-1)}M_o^{\,2}\sin 2\,\sigma}\right]^2} \tag{A3}$$

Equations (A2) and (A3) are the derivatives of the forms of the Rankine-Hugoniot shock relations given in reference 2.

Using the standard forms of the Rankine-Hugoniot shock relations, it is possible to transform equations (3), (4), and (9) (given in the analysis) into

$$\frac{1}{K_w}\frac{dP}{dW} = \frac{\gamma \tan\beta}{\sin^2\alpha}\left[\frac{1 + \frac{1}{2}\left(\frac{\cos^2\alpha}{\cos^2\beta} + \frac{1}{M_o^2\sin^2\sigma}\right)}{\frac{\tan^2\beta}{\tan^2\alpha} + \frac{1}{2}\left(\frac{\cos^2\alpha}{\cos^2\beta} + \frac{1}{M_o^2\sin^2\sigma}\right)}\right]\frac{2\gamma M_o^2\sin^2\sigma - (\gamma-1)}{\gamma+1} \tag{A4}$$

for the surface-pressure gradient,

$$\frac{K_s}{K_w} = \frac{\gamma+1}{4\cos\beta}\left[\frac{1 - \frac{\tan^2\beta}{\tan^2\alpha}}{\frac{\tan^2\beta}{\tan^2\alpha} + \frac{1}{2}\left(\frac{\cos^2\alpha}{\cos^2\beta} + \frac{1}{M_o^2\sin^2\sigma}\right)}\right] \tag{A5}$$

for the shock-wave curvature, and

$$\psi = \left[\frac{1 + \frac{1}{2}\left(\frac{\cos^2\alpha}{\cos^2\beta} + \frac{1}{M_o^2\sin^2\sigma}\right)}{\frac{\tan^2\beta}{\tan^2\alpha} + \frac{1}{2}\left(\frac{\cos^2\alpha}{\cos^2\beta} + \frac{1}{M_o^2\sin^2\sigma}\right)}\right]\frac{\tan\beta}{\tan\alpha} \tag{A6}$$

for the surface-pressure-gradient ratio. These equations are similar to those given by Schaefer in reference 3 and require less work to compute than equations (3), (4), and (9).

For a calorically imperfect, diatomic gas, the standard shock relations obviously are not applicable. However, expressions for the relations for flow of a calorically imperfect gas through an oblique shock wave have been developed in reference 5.

Thus we have, as a function of the local static temperature and free-stream conditions

$$\gamma = \gamma_i \frac{1 + \frac{\gamma_i - 1}{\gamma_i}\left[\left(\frac{\theta}{T}\right)^2 \frac{e^{\theta/T}}{\left(1 - e^{\theta/T}\right)^2}\right]}{1 + (\gamma_i - 1)\left[\left(\frac{\theta}{T}\right)^2 \frac{e^{\theta/T}}{\left(1 - e^{\theta/T}\right)^2}\right]} \tag{A7}$$

where $\gamma_i = 1.400$ and $\theta = 5500^\circ$ R.

The Mach number immediately downstream of the shock can be written

$$M_s^2 = \frac{2}{\gamma_s}\left(\frac{T_o}{T_s}\right)\left[\frac{\gamma_o M_o^2}{2} + \frac{\gamma_i}{\gamma_i - 1}\left(1 - \frac{T_s}{T_o}\right) + \frac{\theta}{T_o}\left(\frac{1}{e^{\theta/T_o} - 1} - \frac{1}{e^{\theta/T_s} - 1}\right)\right] \tag{A8}$$

The relations for the pressure and density ratios across the shock are

$$P_s = \frac{2}{(1+\gamma_s M_s^2) - \frac{T_o}{T_s}(1+\gamma_o M_o^2) + \sqrt{\left[(1+\gamma_s M_s^2) - \frac{T_o}{T_s}(1+\gamma_o M_o^2)\right]^2 + \frac{4\,T_o}{T_s}}} \tag{A9}$$

and

$$\frac{1}{\rho_s} = \frac{T_s}{T_o P_s} \tag{A10}$$

respectively. The expressions for the shock-wave angle and the flow deflection angle are

$$\sin^2\sigma = \frac{\frac{\gamma_s}{\gamma_o}\frac{T_s}{T_o}\left(\frac{M_s}{M_o}\right)^2 - 1}{\left(\frac{1}{\rho_s}\right)^2 - 1} \tag{A11}$$

and

$$\cot\delta_s = \tan\sigma\left(\frac{\gamma_o M_o^2}{P_s - 1} - 1\right) \tag{A12}$$

respectively. Equations (A7) through (A12) are valid for temperatures downstream of the shock wave up to the order of 5000° R.

The primary variable is the temperature immediately downstream of the shock wave. Hence, we can write

$$(dP/d\delta)_s = \frac{(dP/dT)_s}{(d\delta/dT)_s} \tag{A13}$$

and

$$(d\delta/d\sigma)_s = \frac{(d\delta/dT)_s}{(d\sigma/dT)_s} \tag{A14}$$

Differentiation of equation (A9) yields

$$\left(\frac{dP}{dT}\right)_s = -2\left\{\frac{\left[2\gamma_s M_s\left(\frac{dM}{dT}\right)_s + M_s^2\left(\frac{d\gamma}{dT}\right)_s + \left(1+\gamma_o M_o^2\right)\frac{T_o}{T_s^2}\right]}{\left[F + \sqrt{F^2 + \frac{4T_o}{T_s}}\right]^2} + \frac{F\left[2\gamma_s M_s\left(\frac{dM}{dT}\right)_s + M_s^2\left(\frac{d\gamma}{dT}\right)_s + \left(1+\gamma_o M_o^2\right)\frac{T_o}{T_s^2}\right] - 2\frac{T_o}{T_s^2}}{\left[F + \sqrt{F^2 + \frac{4T_o}{T_s}}\right]^2\sqrt{F^2 + \frac{4T_o}{T_s}}}\right\} \tag{A15}$$

where $F = 1 + \gamma_s M_s^2 - \frac{T_o}{T_s}\left(1 + \gamma_o M_o^2\right)$

where

$$\left(\frac{dM}{dT}\right)_s = \frac{-\dfrac{\gamma_i}{\gamma_s(\gamma_i-1)T_s} - \dfrac{\left(\dfrac{\theta^2}{T_s^3}\right)e^{\theta/T_s}}{\gamma_s\left(e^{\theta/T_s}-1\right)^2} - \left[\dfrac{1}{T_s} + \dfrac{1}{\gamma_s}\left(\dfrac{d\gamma}{dT}\right)_s\right]\left\{\dfrac{T_o}{\gamma_s T_s}\left[\dfrac{\gamma_o M_o^2}{2} + \dfrac{\gamma_i}{\gamma_i-1}\left(1-\dfrac{T_s}{T_o}\right) + \dfrac{\theta}{T_o}\left(\dfrac{1}{e^{\theta/T_o}-1} - \dfrac{1}{e^{\theta/T_s}-1}\right)\right]\right\}}{\sqrt{\dfrac{2}{\gamma_s}\left(\dfrac{T_o}{T_s}\right)\left[\dfrac{\gamma_o M_o^2}{2} + \dfrac{\gamma_i}{\gamma_i-1}\left(1-\dfrac{T_s}{T_o}\right) + \dfrac{\theta}{T_o}\left(\dfrac{1}{e^{\theta/T_o}-1} - \dfrac{1}{e^{\theta/T_s}-1}\right)\right]}} \tag{A16}$$

and

$$\left(\frac{d\gamma}{dT}\right)_s = -\gamma_i\left[\frac{\dfrac{\gamma_i-1}{\gamma_i}\left[\left(-1+e^{\theta/T_s}\right)\left(\dfrac{\theta^3}{T_s^4}+\dfrac{2\theta^2}{T_s^3}\right)e^{\theta/T_s} - 2\left(\dfrac{\theta^3}{T_s^4}\right)e^{2\theta/T_s}\right]}{\left\{1+(\gamma_i-1)\left[\left(\dfrac{\theta}{T_s}\right)^2\dfrac{e^{\theta/T_s}}{\left(-1+e^{\theta/T_s}\right)^2}\right]\right\}\left(-1+e^{\theta/T_s}\right)^3} - \frac{\left\{1+\dfrac{(\gamma_i-1)}{\gamma_i}\left[\left(\dfrac{\theta}{T_s}\right)^2\dfrac{e^{\theta/T_s}}{\left(-1+e^{\theta/T_s}\right)^2}\right]\right\}(\gamma_i-1)\left[\left(-1+e^{\theta/T_s}\right)\left(\dfrac{\theta^3}{T_s^4}+\dfrac{2\theta^2}{T_s^3}\right)e^{\theta/T_s} - 2\dfrac{\theta^3}{T_s^4}e^{2\theta/T_s}\right]}{\left\{1+(\gamma_i-1)\left[\left(\dfrac{\theta}{T_s}\right)^2\dfrac{e^{\theta/T_s}}{\left(-1+e^{\theta/T_s}\right)^2}\right]\right\}^2\left(-1+e^{\theta/T_s}\right)^3}\right] \tag{A17}$$

Equations (A16) and (A17) are obtained by differentiating equations (A8) and (A7), respectively. Similarly, differentiation of equation (A12) yields

$$\left(\frac{d\delta}{dT}\right)_s = -\sin^2\delta\left\{\frac{\tan\sigma\left[-\gamma_o M_o^2\left(\dfrac{dP}{dT}\right)_s\right]}{(P_s-1)^2} + \left(\frac{\gamma_o M_o^2}{P_s-1} - 1\right)\sec^2\sigma\left(\frac{d\sigma}{dT}\right)_s\right\} \tag{A18}$$

where

$$\left(\frac{d\sigma}{dT}\right)_s = \frac{\left[\left(\frac{1}{\rho}\right)_s^2 - 1\right]\left\{\frac{\gamma_s}{\gamma_o}\left[\frac{1}{T_o}\left(\frac{M_s}{M_o}\right)^2 + \frac{T_s}{T_o}\left(\frac{2M_s}{M_o^2}\right)\left(\frac{dM}{dT}\right)_s\right] + \frac{T_s}{\gamma_o T_o}\left(\frac{M_s}{M_o}\right)^2\left(\frac{d\gamma}{dT}\right)_s\right\} - \left[\frac{\gamma_s}{\gamma_o}\frac{T_s}{T_o}\left(\frac{M_s}{M_o}\right)^2 - 1\right]\left\{\frac{2}{\rho_s}\left[\frac{d\left(\frac{1}{\rho}\right)}{dT}\right]_s\right\}}{2 \sin\sigma \cos\sigma \left[\left(\frac{1}{\rho_s}\right)^2 - 1\right]^2} \tag{A19}$$

and

$$\left[\frac{d\left(\frac{1}{\rho}\right)}{dT}\right]_s = \frac{1}{P_s T_o} - \frac{T_s}{T_o P_s^2}\left(\frac{dP}{dT}\right)_s \tag{A20}$$

The procedure for calculating $\frac{1}{K_w}\frac{dP}{dW}$, $\frac{K_s}{K_w}$, ψ, and κ is straightforward with the aid of the preceding equations and may be summarized as follows:

1. For any M_o, K_w, and δ_N, choose T_o and T_s/T_o. An approximate value of T_s/T_o may be obtained from figure 11.

2. Calculate γ_s (equation (A7))

3. Calculate M_s (equation (A8))

4. Calculate P_s (equation (A9))

5. Calculate $\frac{1}{\rho_s}$ (equation (A10))

6. Calculate σ_N (equation (A11))

7. Calculate δ_s (equation (A12))

If this value of δ_s is not close enough to the desired value of δ_N, iterate, choosing a new T_s/T_o.

8. Calculate $\left(\frac{d\gamma}{dT}\right)_s$ (equation (A17))
9. Calculate $\left(\frac{d\hat{M}}{dT}\right)_s$ (equation (A16))
10. Calculate $\left(\frac{dP}{dT}\right)_s$ (equation (A15))
11. Calculate $\left[\frac{d(1/\rho)}{dT}\right]_s$ (equation (A20))
12. Calculate $\left(\frac{d\sigma}{dT}\right)_s$ (equation (A19))
13. Calculate $\left(\frac{d\delta}{dT}\right)_s$ (equation (A18))
14. Calculate $\left(\frac{dP}{d\delta}\right)_s$ (equation (A13))
15. Calculate $\left(\frac{d\delta}{dP}\right)_{C_2}$ (equation (2))
16. Calculate Z (equation (5))
17. Calculate $\frac{1}{K_w}\frac{dP}{dW}$ (equation (3))
18. Calculate ψ (equation (9))
19. Calculate $\left(\frac{d\delta}{d\sigma}\right)_s$ (equation (A14))
20. Calculate $\frac{K_s}{K_w}$ (equation (4))
21. Calculate κ (equation (10))

REFERENCES

1. Crocco, Luigi: Singolarita della Corrente Gassosa Iperacustica Nell'Intorno di una Prora a Diedro. L'Aerotecnica, vol. 17, no. 6, June 1937.

2. Munk, M. M., and Prim, R. C.: Surface-Pressure Gradient and Shock Front Curvature at the Edge of a Plane Ogive with Attached Shock Front. Jour. Inst. Aero. Sci., vol. 15, no. 11, Nov. 1948, pp. 691-695.

3. Schaefer, M.: The Relation Between Wall Curvature and Shock Front Curvature in Two Dimensional Gas Flow. A.F., AMC, Tech. Rept. F-TS-1202-IA. (GDAM A9-T-9) Brown University. (Technische Hochschule Dresden, 1942. Peenemunde Archiv 44/8.)

4. Thomas, T. Y.: Calculation of the Curvature of Attached Shock Waves. Jour. Math. and Physics, vol. 27, no. 4, Jan. 1949, pp. 279-297.

5. Eggers, A. J., Jr., and Syvertson, Clarence A.: Inviscid Flow About Airfoils at High Supersonic Speeds. NACA TN 2646, 1952.

6. Eggers, A. J., Jr.: One-Dimensional Flows of an Imperfect Diatomic Gas. NACA Rep. 959, 1950. (Formerly NACA TN 1861, 1949)

7. Bethe, H. A., and Teller, E.: Deviations from Thermal Equilibrium in Shock Waves. Aberdeen Proving Ground, Maryland. Ballistic Research Lab. Rep. No. X-117, 1945.

TABLE I.- SURFACE-PRESSURE GRADIENT

Surface-pressure gradient, $\frac{1}{K_W}\frac{dP}{dW}$											
δ_N \ M_o	1.5	2.0	3.0	4.0	5.0	6.0	8.0	10.0	15.0	20.0	∞
0°	2.8175	3.2332	4.4550	5.7827	7.1426	8.5226	11.2897	14.0686	21.0460	28.0350	∞
2.0°	3.0893	3.5297	5.0384	6.8091	8.7576	10.8700	15.5882	20.9907	37.7826	59.8143	∞
5.0°	3.6146	4.0135	6.0077	8.5769	11.6359	15.1989	23.9418	35.0225	74.0084	130.205	∞
7.5°	4.2985	4.4580	6.8962	10.2428	14.4132	19.4482	32.2994	49.1026	109.319	195.900	∞
10.0°	5.8776	4.9502	7.8492	12.0538	17.4590	24.1212	41.4247	64.2295	145.662	261.647	∞
15.0°		6.1853	9.9078	15.9604	24.0001	34.0605	60.3209	94.7569	216.102	387.105	∞
20.0°		8.7654	12.1185	19.9892	30.5936	43.8720	78.3454	123.225	280.229	500.683	∞
25.0°			14.5607	23.9362	36.7961	52.8797	94.4435	148.323	336.203	599.631	∞
30.0°			18.2498	27.9349	42.5428	60.9129	108.339	169.705	383.415	682.891	∞
35.0°				33.8949	48.8338	68.8023	120.915	188.457	423.792	753.506	∞
40.0°					71.7623	84.9024	139.218	212.761	471.107	833.770	∞
45.0°									1727.39	1711.33	∞

NACA

TABLE II.- SURFACE-PRESSURE-GRADIENT RATIO

Surface-pressure-gradient ratio, ψ											
δ_N \ M_o	1.5	2.0	3.0	4.0	5.0	6.0	8.0	10.0	15.0	20.0	∞
0°	1.00000	1.00000	1.00000	1.00000	1.00000	1.00000	1.00000	1.00000	1.00000	1.00000	.88200
2.0°	1.00003	1.00001	.99999	.99996	.99992	.99984	.99962	.99927	.99762	.99477	.88200
5.0°	1.00039	1.00012	.99984	.99942	.99874	.99779	.99497	.99097	.97728	.96181	.88218
7.5°	1.00134	1.00046	.99948	.99814	.99614	.99348	.98638	.97773	.95497	.93622	.88251
10.0°	.99781	1.00118	.99883	.99594	.99197	.98704	.97535	.96305	.93693	.91979	.88305
15.0°		1.00561	.99696	.98947	.98076	.97150	.95428	.93913	.91583	.90411	.88462
20.0°		1.02497	.99582	.98244	.96961	.95779	.93868	.92528	.90714	.89914	.88717
25.0°			.99972	.97831	.96225	.94932	.93090	.91939	.90521	.89942	.89117
30.0°			1.02540	.98254	.96218	.94820	.93049	.92036	.90872	.90417	.89790
35.0°				1.01645	.97870	.96029	.94073	.93066	.91990	.91585	.91042
40.0°					1.11404	1.02772	.98347	.96724	.95228	.94718	.94066
45.0°									1.73742	1.32519	1.18808

TABLE III.- SHOCK-WAVE CURVATURE

Shock-wave curvature, K_s/K_w											
δ_N \ M_o	1.5	2.0	3.0	4.0	5.0	6.0	8.0	10.0	15.0	20.0	∞
0°	0	0	0	0	0	0	0	0	0	0	0.80000
2.0°	.065969	.045475	.048052	.057669	.068912	.080794	.10542	.13051	.19314	.25373	.80024
5.0°	.19513	.11748	.12117	.14497	.17278	.20179	.25987	.31557	.43574	.52642	.80185
7.5°	.36983	.18267	.18275	.21696	.25659	.29688	.37332	.44059	.56524	.64172	.80425
10.0°	.79882	.25534	.24470	.28694	.33539	.38294	.46763	.53568	.64596	.70424	.80764
15.0°		.44870	.37040	.41833	.47374	.52442	.60443	.65972	.73454	.76779	.81815
20.0°		.91907	.50509	.53988	.58947	.63325	.69700	.73702	.78626	.80646	.83520
25.0°			.67561	.66337	.69563	.72708	.77233	.79964	.83183	.84451	.86212
30.0°			1.01371	.82220	.81683	.82937	.85366	.86952	.88850	.89604	.90643
35.0°				1.16770	1.02118	.98902	.97730	.97794	.98180	.98403	.98750
40.0°					2.03983	1.49218	1.29256	1.23976	1.20180	1.19114	1.17917
45.0°									7.66889	3.82862	2.81101

TABLE IV.- SHOCK-WAVE-CURVATURE RATIO

Shock-wave-curvature Ratio, κ											
δ_N \ M_o	1.5	2.0	3.0	4.0	5.0	6.0	8.0	10.0	15.0	20.0	∞
0°	1.0000	1.0000	1.0000	1.0000	1.0000	1.0000	1.0000	1.0000	1.0000	1.0000	1.0718
2.0°	.99947	.99987	1.0004	1.0004	1.0007	1.0011	1.0021	1.0034	1.0062	1.0122	1.0717
5.0°	.99833	.99927	1.0008	1.0025	1.0043	1.0066	1.01148	1.0171	1.0297	1.0401	1.0715
7.5°	.99699	.99825	1.0018	1.0052	1.0090	1.0131	1.02118	1.0289	1.0436	1.0526	1.0712
10.0°	1.0024	.99679	1.0030	1.0086	1.0142	1.0199	1.03007	1.0384	1.0519	1.0589	1.0706
15.0°		.99117	1.0051	1.0150	1.0236	1.0309	1.04203	1.0495	1.0590	1.0631	1.0691
20.0°		.97958	1.0052	1.0192	1.0295	1.0372	1.04737	1.0533	1.0602	1.0630	1.0667
25.0°			1.0003	1.0194	1.0309	1.0386	1.04785	1.0528	1.0582	1.0603	1.0630
30.0°			.9830	1.0128	1.0266	1.0348	1.04389	1.0484	1.0532	1.0550	1.0573
35.0°				.99084	1.0126	1.0232	1.03362	1.0387	1.0435	1.0453	1.0476
40.0°					.95871	.98788	1.00774	1.0155	1.0227	1.0252	1.0282
45.0°									.88547	.92416	.94753

NACA

TABLE V.- SURFACE-PRESSURE GRADIENT, SURFACE-PRESSURE-GRADIENT RATIO, SHOCK-WAVE CURVATURE, AND SHOCK-WAVE-CURVATURE RATIO FOR A CALORICALLY IMPERFECT, DIATOMIC GAS [T_o = 500° RANKINE]

Mo	δ^o	T_s/T_o	$\frac{1}{K_w}\frac{dP}{dW}$	ψ	K_s/K_w	κ
3	30.4757	2.012	18.36	1.0262	1.0212	0.9828
5	20.4748	2.138	30.94	.9675	.5866	1.0312
5	31.0968	3.127	42.63	.9548	.7987	1.0313
5	41.0064	4.300	60.76	1.0419	1.5991	1.0000
10	10.0129	2.108	63.87	.9622	.5266	1.0394
10	20.5239	4.400	123.6	.9111	.7137	1.0621
10	31.2637	7.640	169.8	.8889	.8363	1.0636
10	42.9772	[a]12.000	205.2	.9178	1.1678	1.0365
20	10.6610	4.700	274.1	.9024	.6912	1.0685
20	20.9696	[a]12.600	515.0	.8592	.8041	1.0787
20	32.5087	[a]25.800	705.1	.8492	.8915	1.0753
20	39.1836	[a]35.000	770.4	.8559	.9858	1.0664

[a]Values of temperature greater than 5000° R downstream of the shock wave.

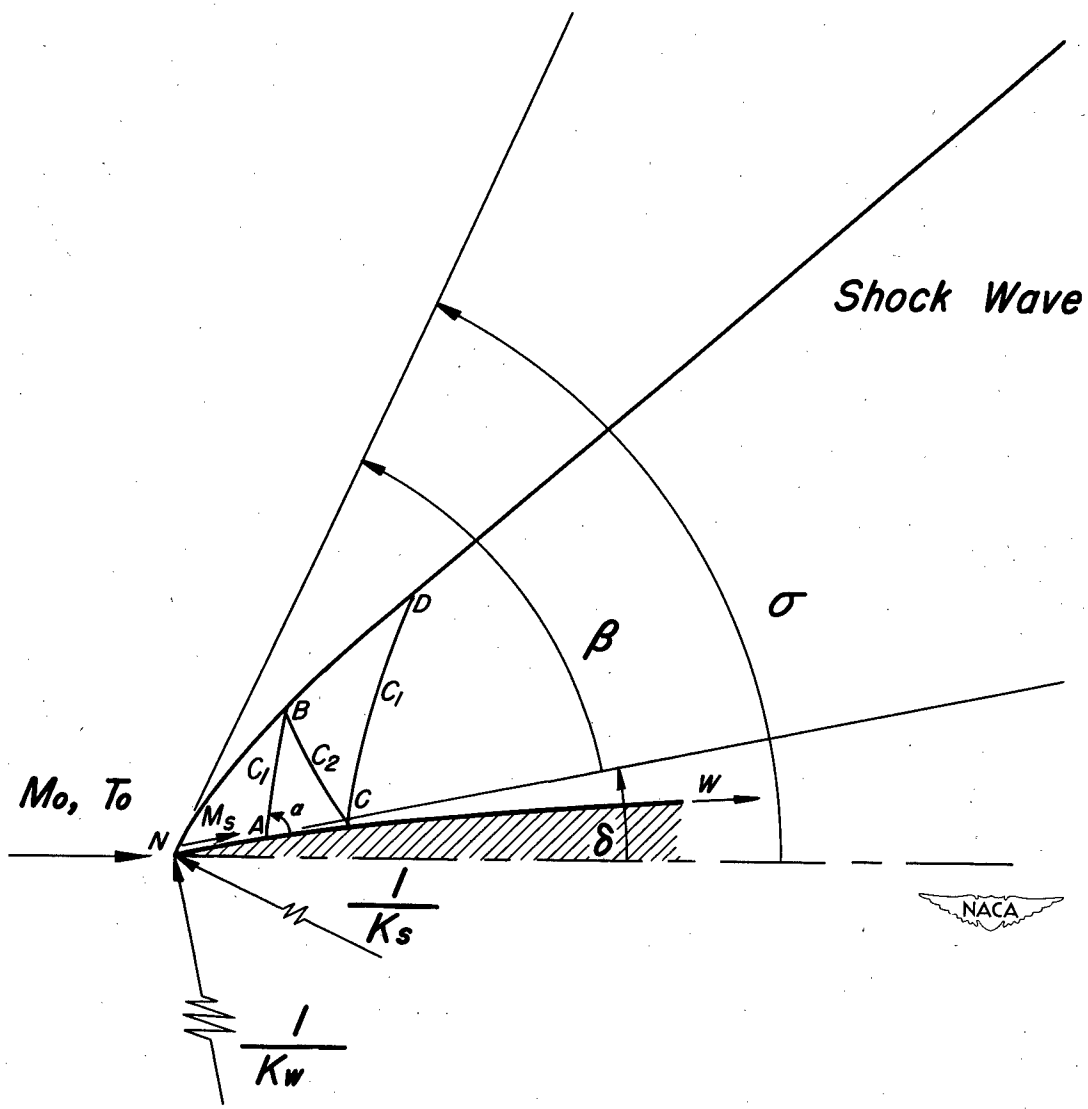

Figure 1.— Schematic diagram of supersonic flow past a curved sharp-nose airfoil.

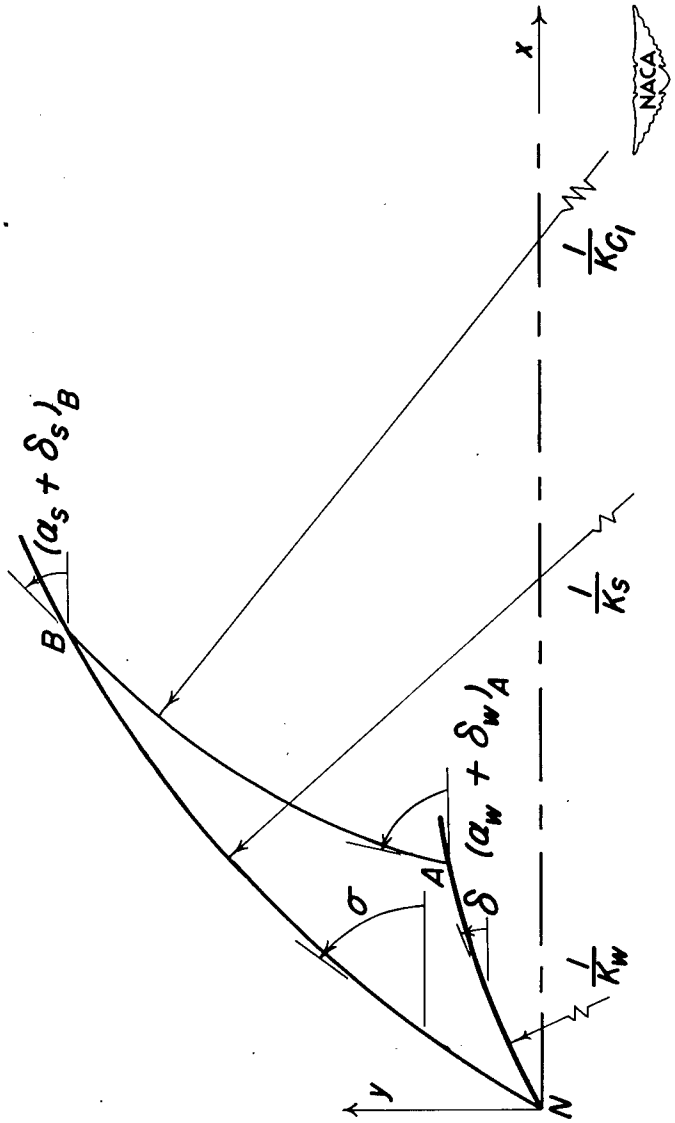

Figure 2.– Nose region with shock wave, airfoil surface, and Mach wave approximated by circular arcs.

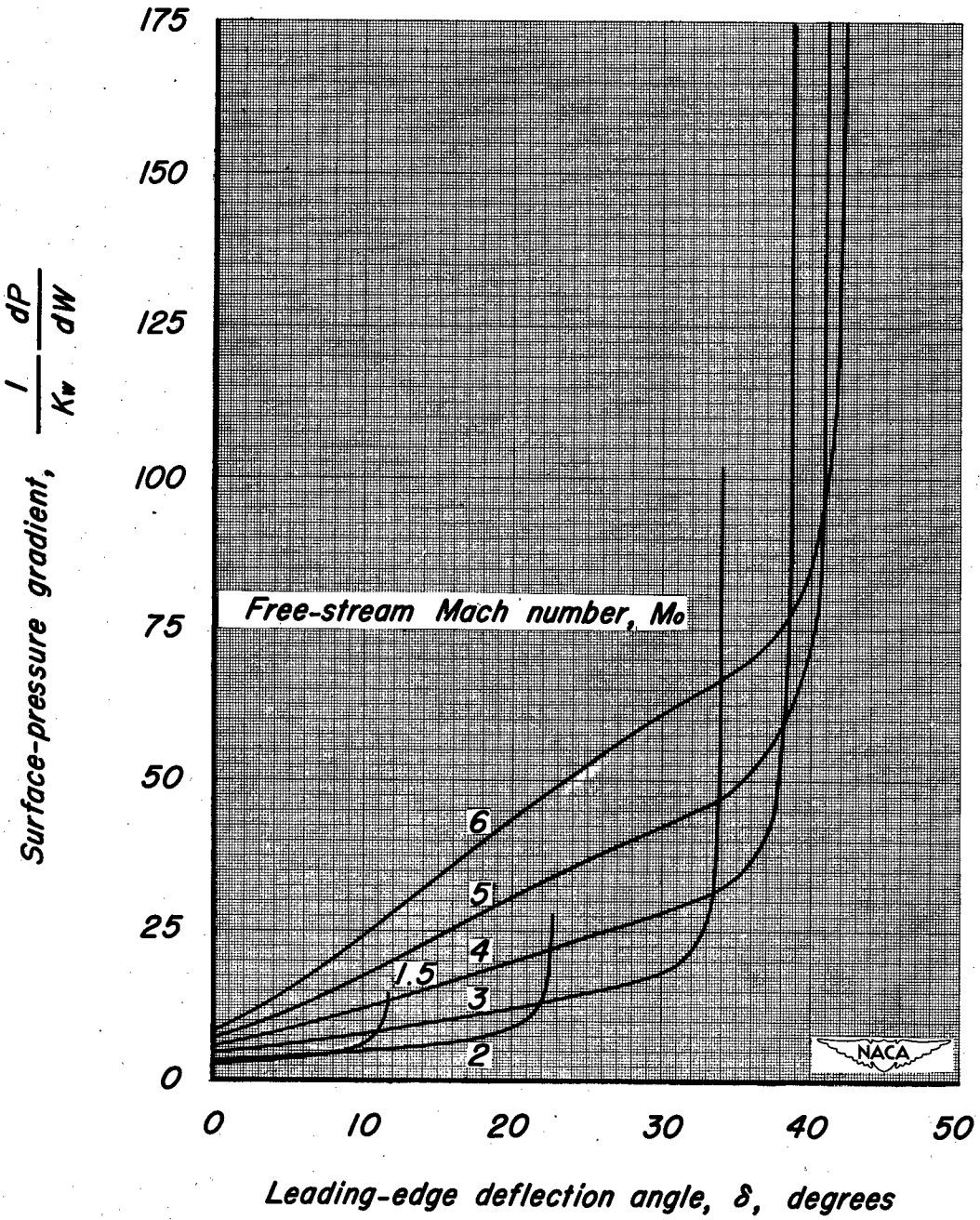

(a) M_0, 1.5 to 6

Figure 3.—Variation of surface-pressure gradient with leading-edge deflection angle for various free-stream Mach numbers.

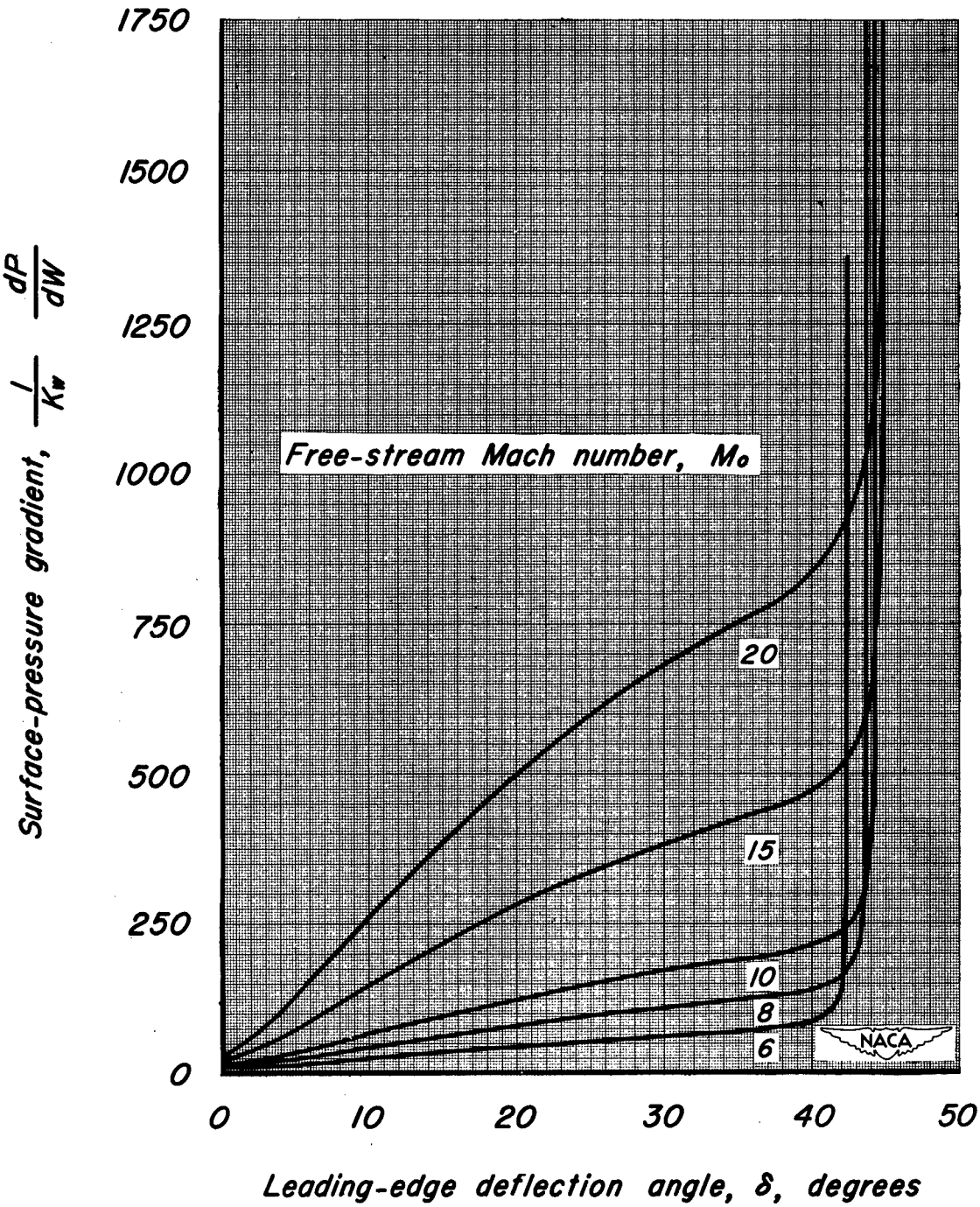

(b) M_o, 6 to 20

Figure 3.—Concluded.

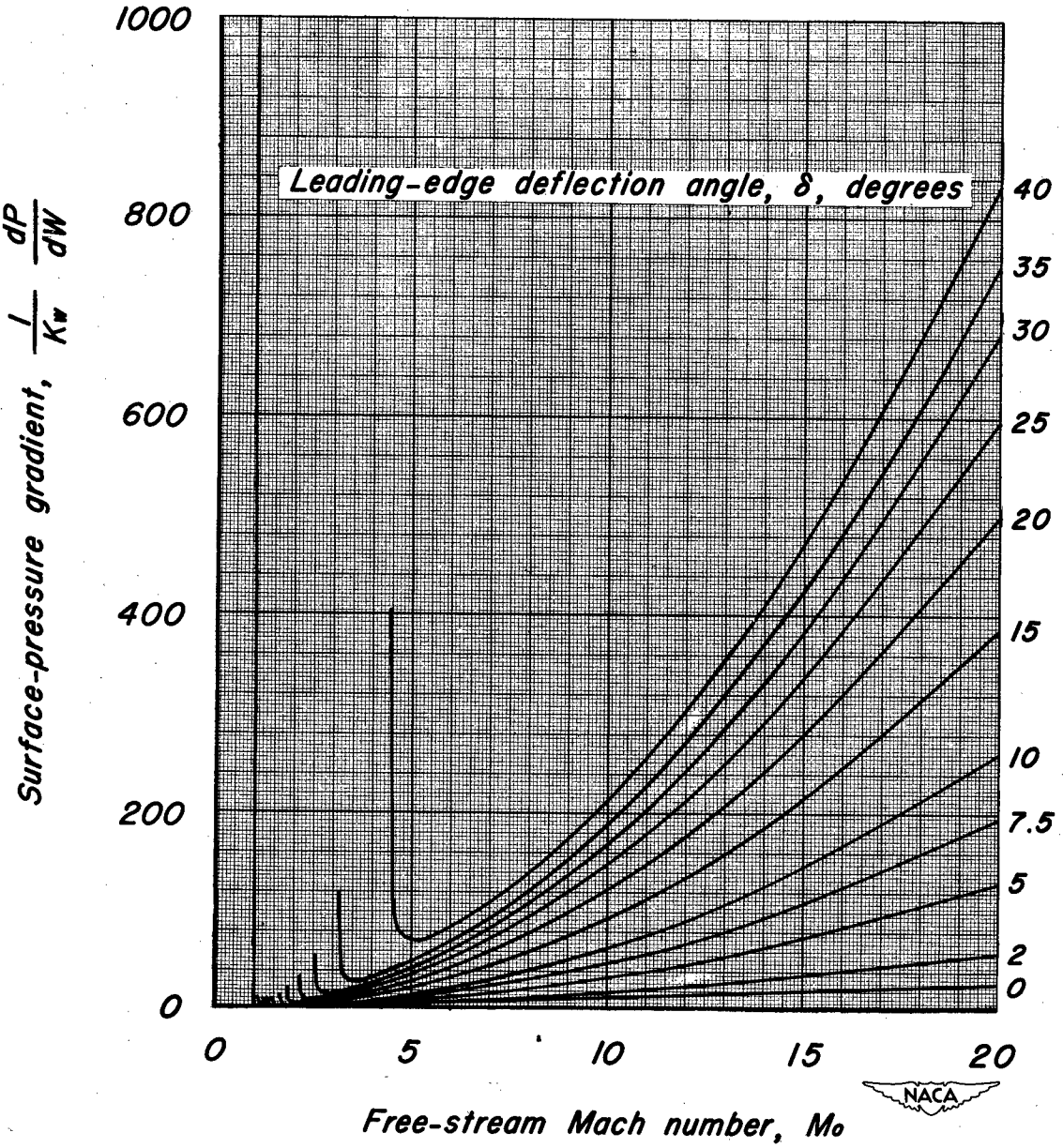

(a) $\frac{1}{K_w}\frac{dP}{dW}$, 0 to 1000

Figure 4.—Variation of surface-pressure gradient with free-stream Mach number for various leading-edge deflection angles.

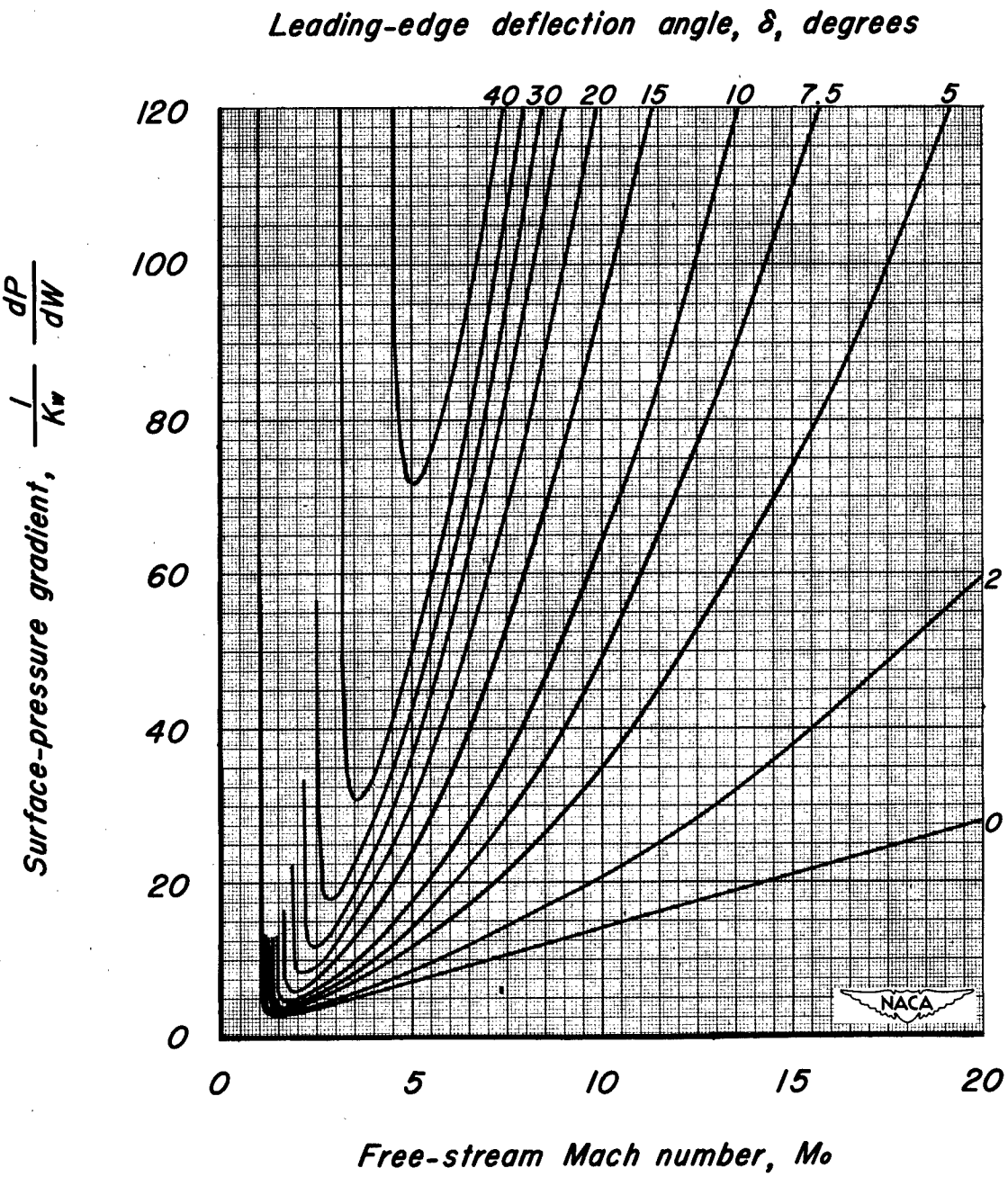

(b) $\frac{1}{K_w}\frac{dP}{dW}$, 0 to 120

Figure 4.—Concluded.

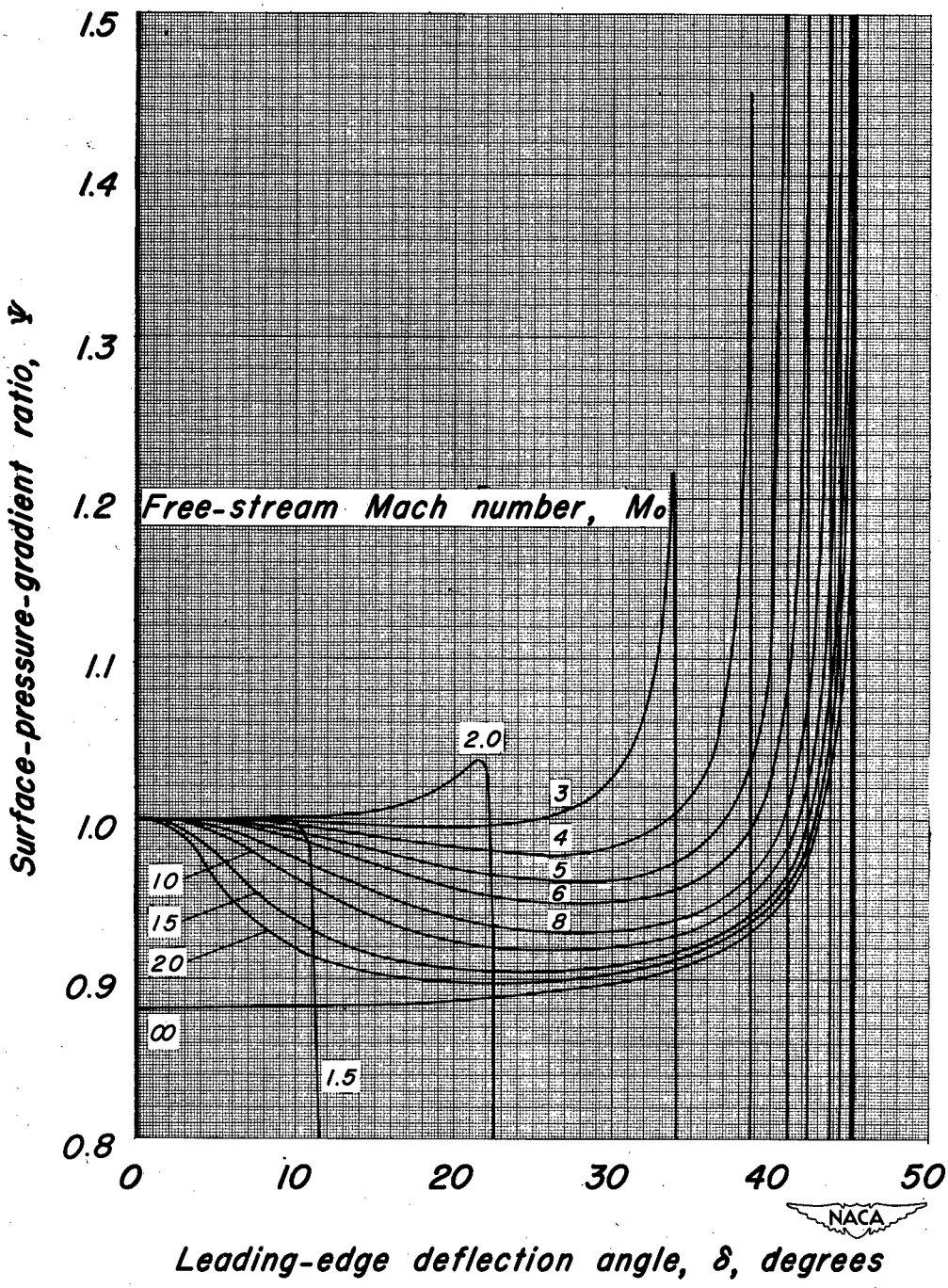

Figure 5.–Variation of surface-pressure-gradient ratio with deflection angle for various free-stream Mach numbers.

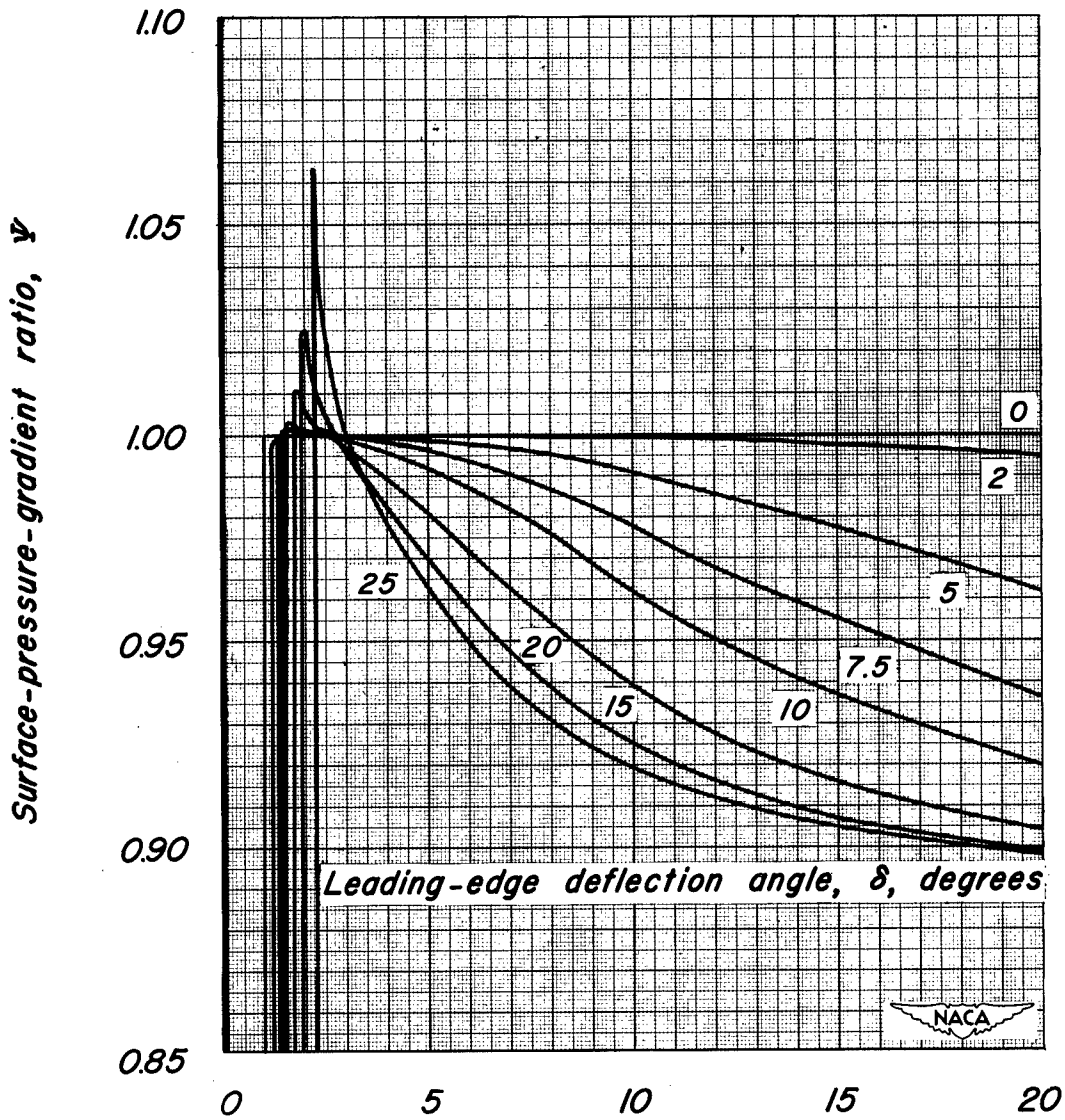

(a) δ, 0° to 25°

Figure 6.- Variation of surface-pressure-gradient ratio with free-stream Mach number for various leading-edge deflection angles.

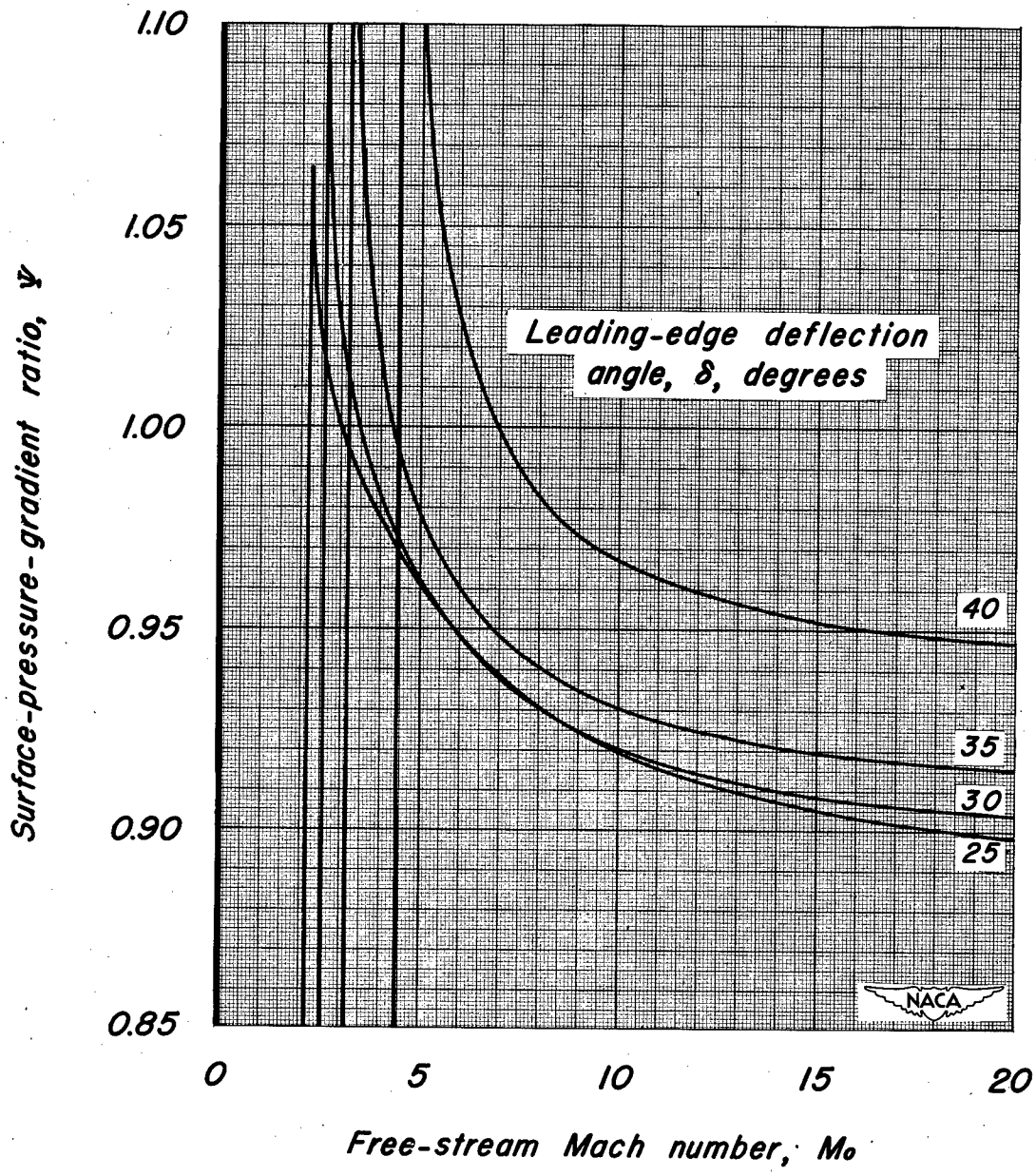

(b) δ, 25° to 40°

Figure 6.- Concluded.

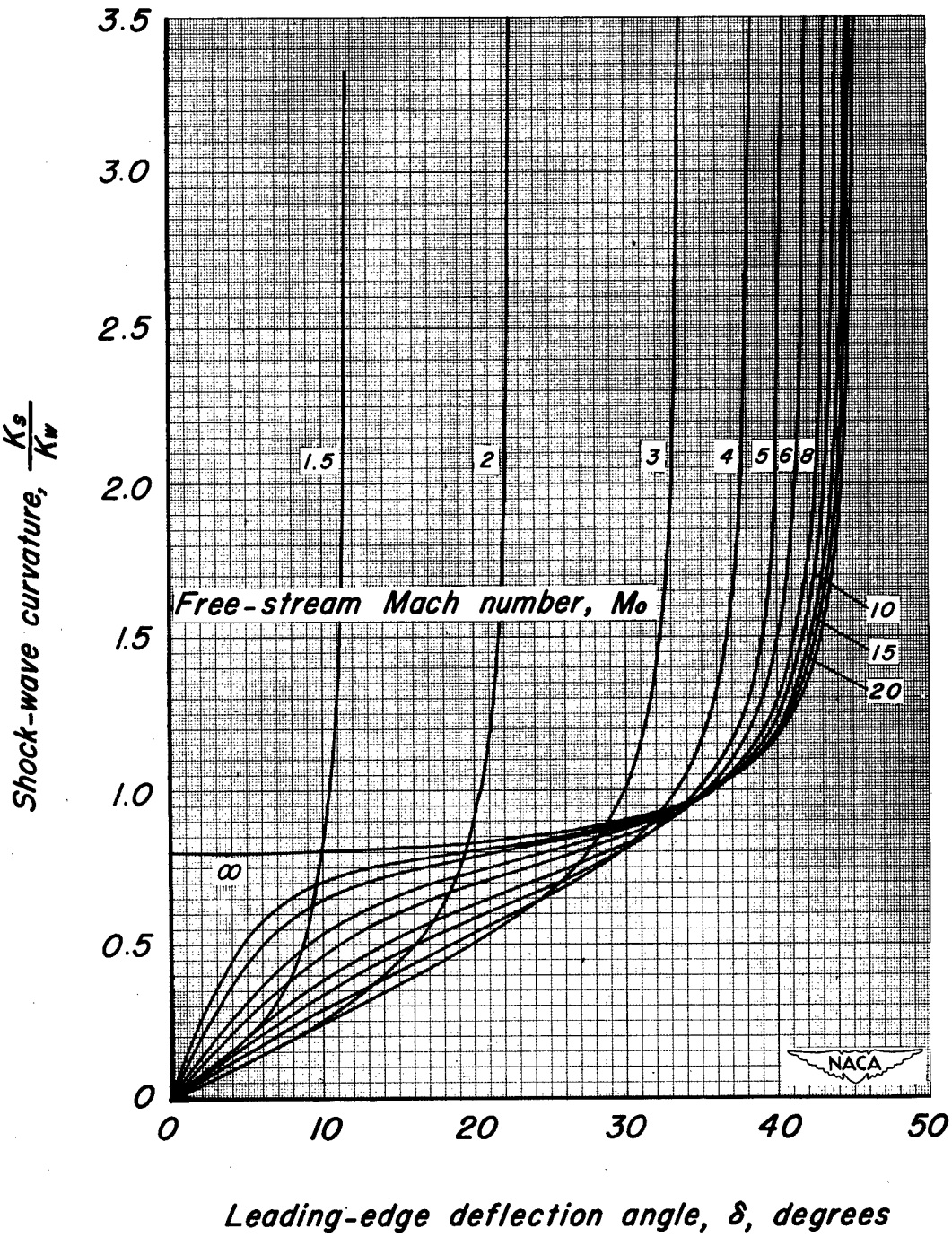

Figure 7.—Variation of shock-wave curvature with leading-edge deflection angle for various free-stream Mach numbers.

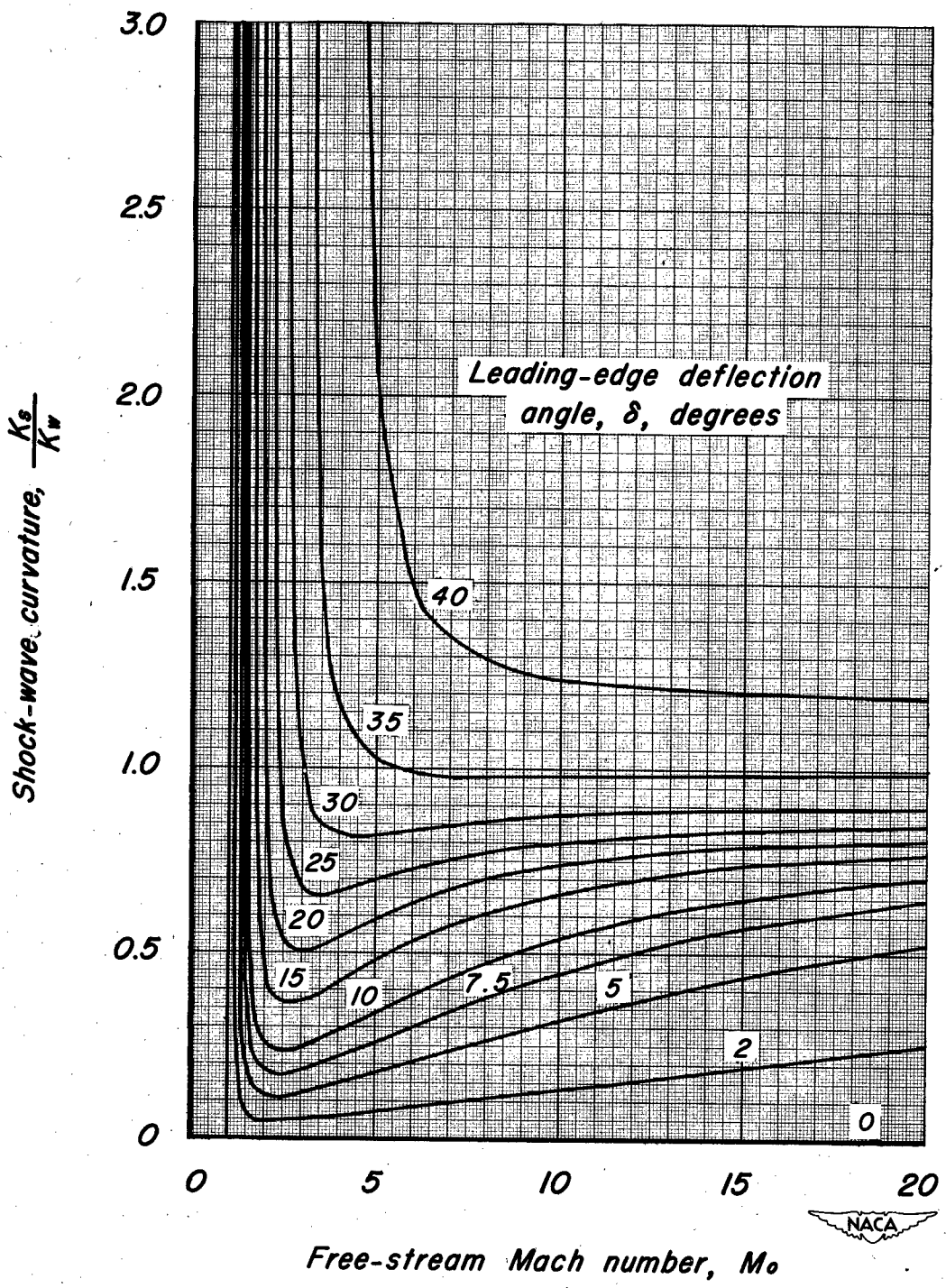

Figure 8.– Variation of shock-wave curvature with free-stream Mach number for various leading-edge deflection angles.

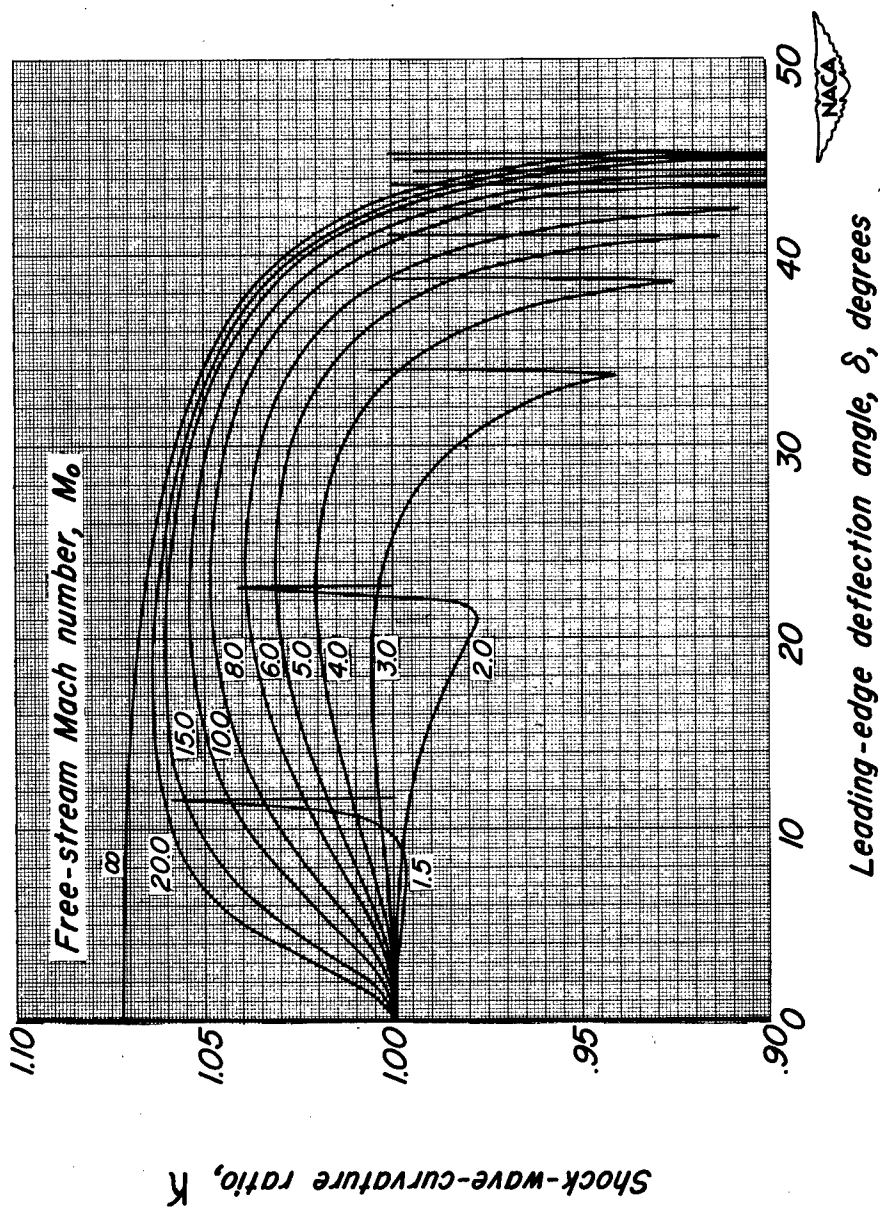

Figure 9.–Variation of shock-wave-curvature ratio with leading-edge deflection angle for various free-stream Mach numbers.

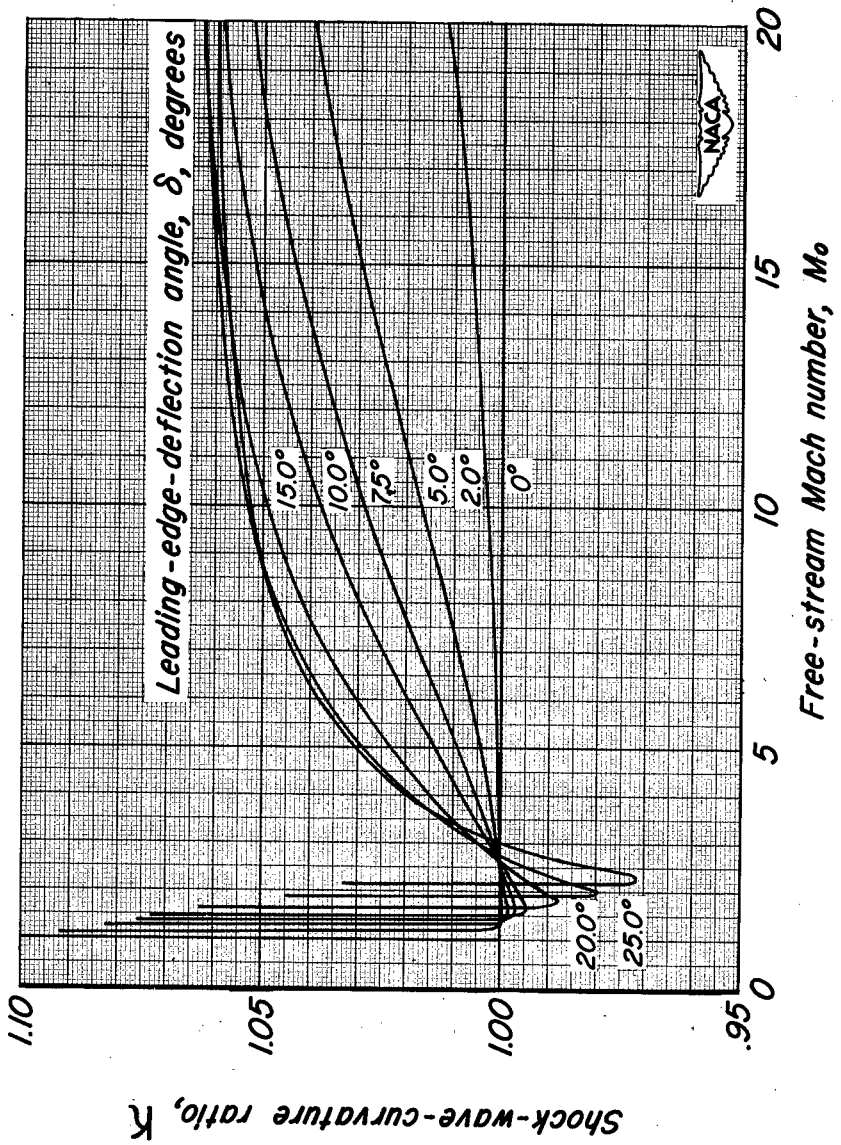

(a) δ, 0° to 25°

Figure 10.–Variation of shock-wave-curvature ratio with free-stream Mach number for various leading-edge deflection angles.

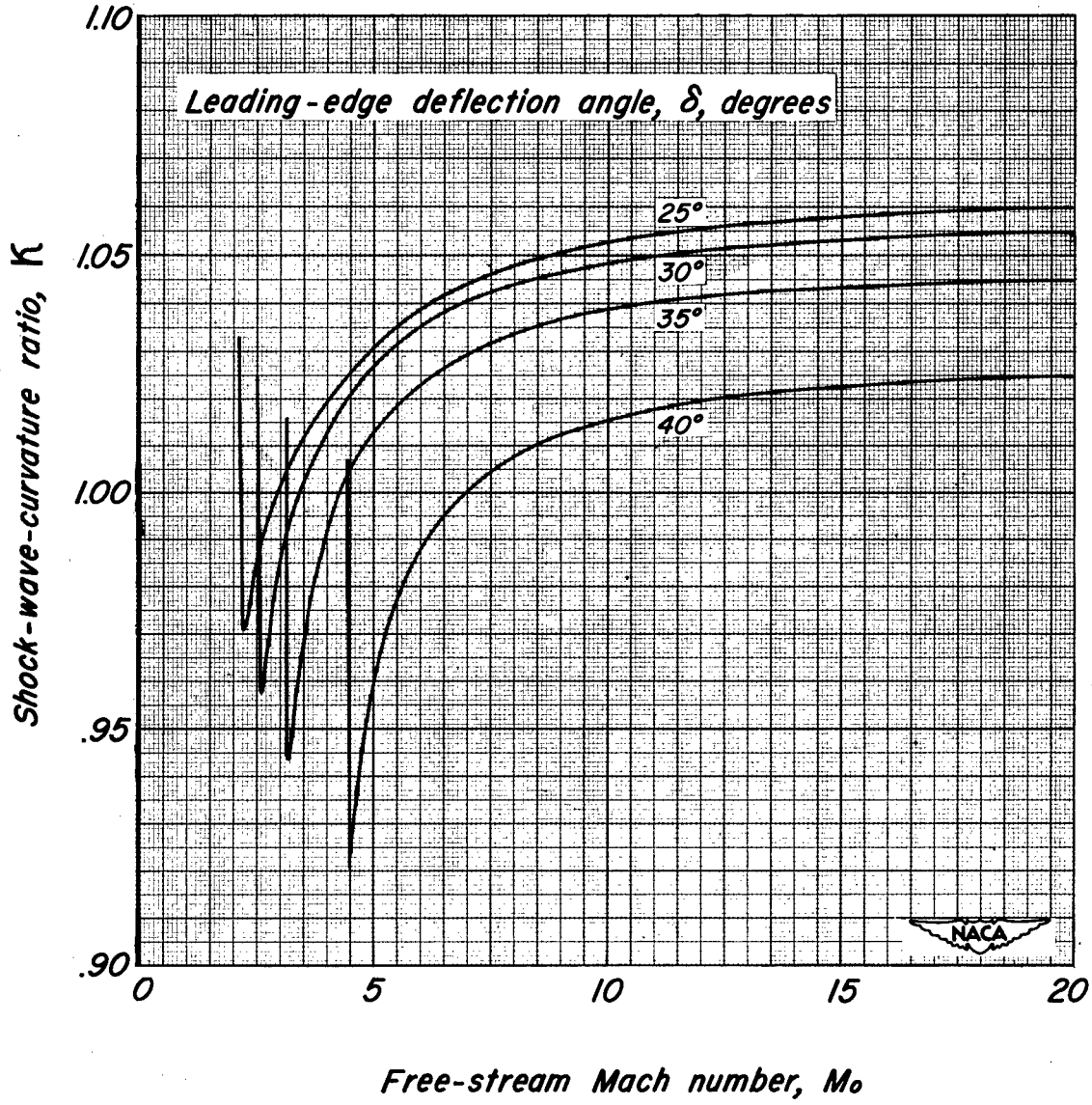

(b) δ, 25° to 40°

Figure 10.–Concluded.

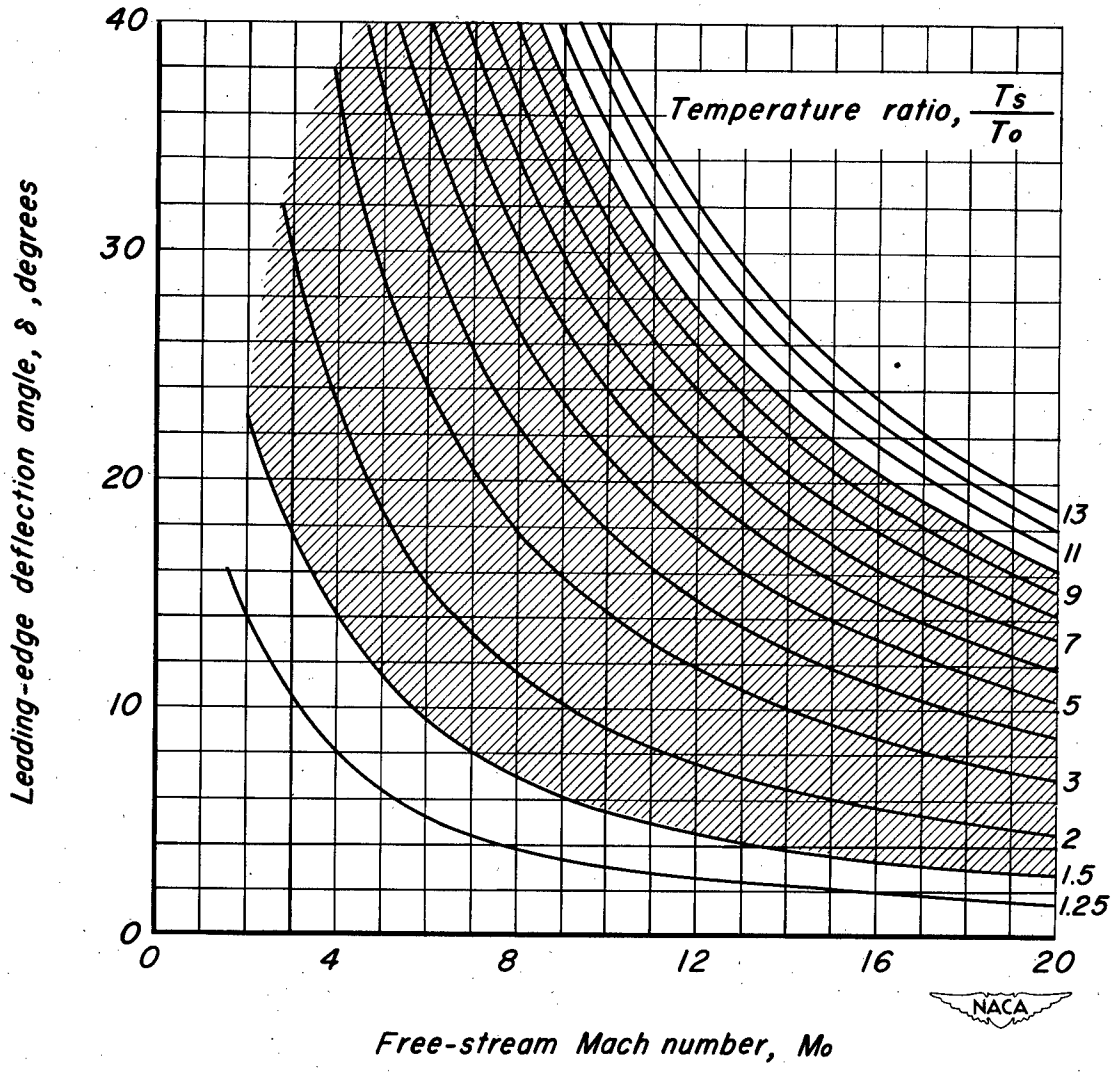

Figure 11.—Variation of leading-edge deflection angle with free-stream Mach number for various values of the temperature ratio.

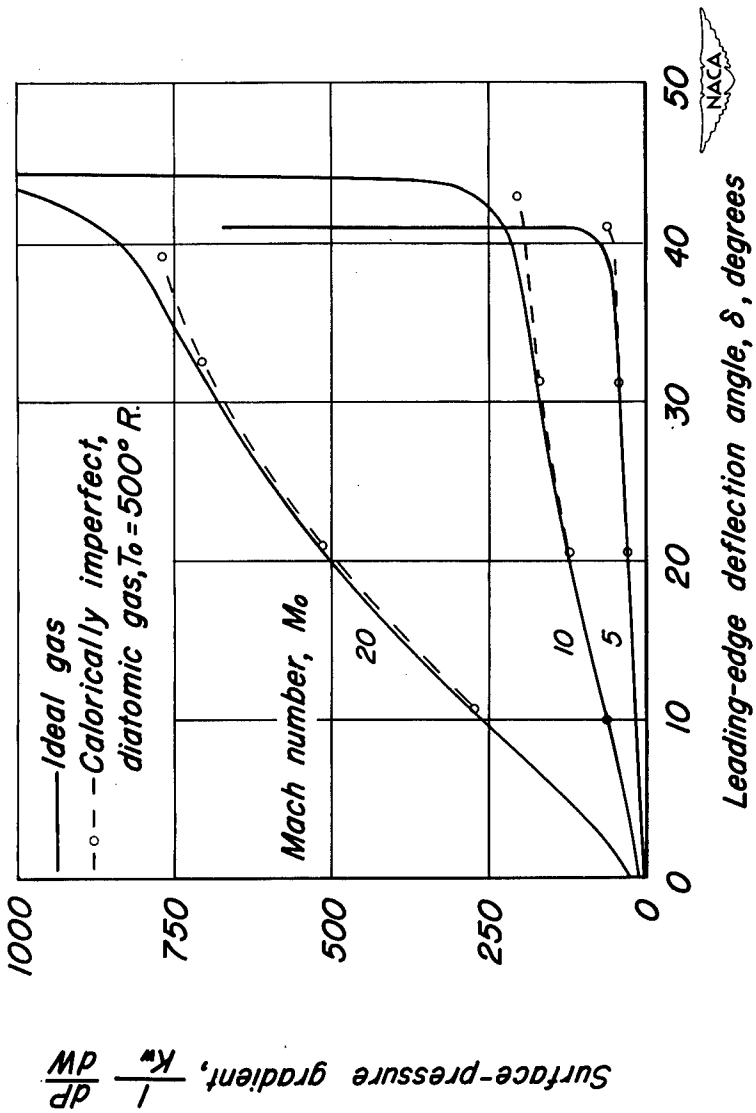

Figure 12.– Comparison of the variation of surface-pressure gradient with leading-edge deflection angle for various free-stream Mach numbers for an ideal gas and for a calorically imperfect, diatomic gas.

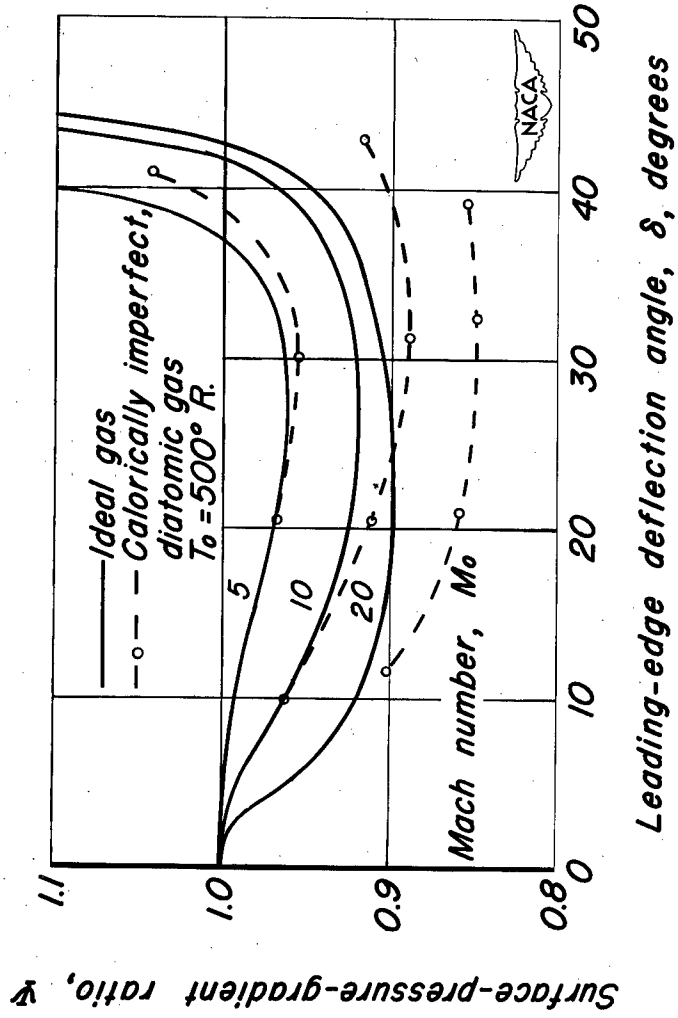

Figure 13.—Comparison of the variation of surface-pressure-gradient ratio with leading-edge deflection angle for various free-stream Mach numbers for an ideal gas and for a calorically imperfect, diatomic gas.

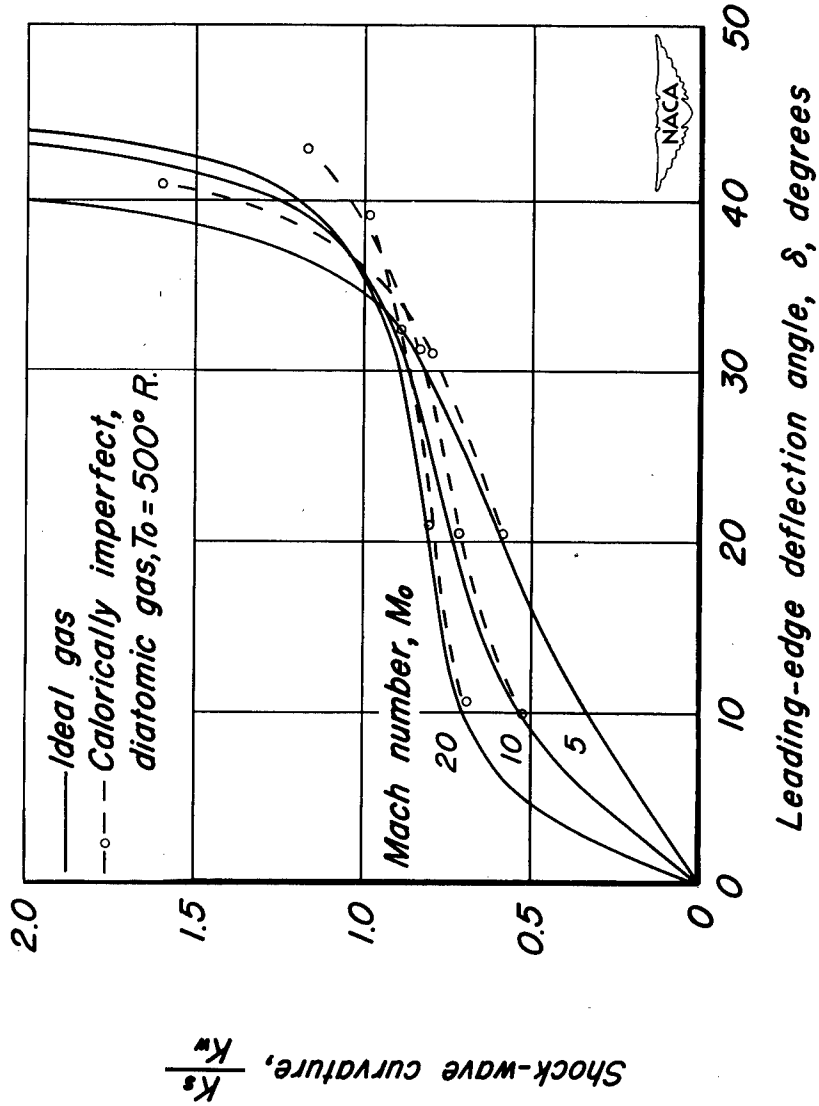

Figure 14.- Comparison of the variation of the shock-wave curvature with the leading-edge deflection angle for various free-stream Mach numbers for an ideal gas and for a calorically imperfect, diatomic gas.

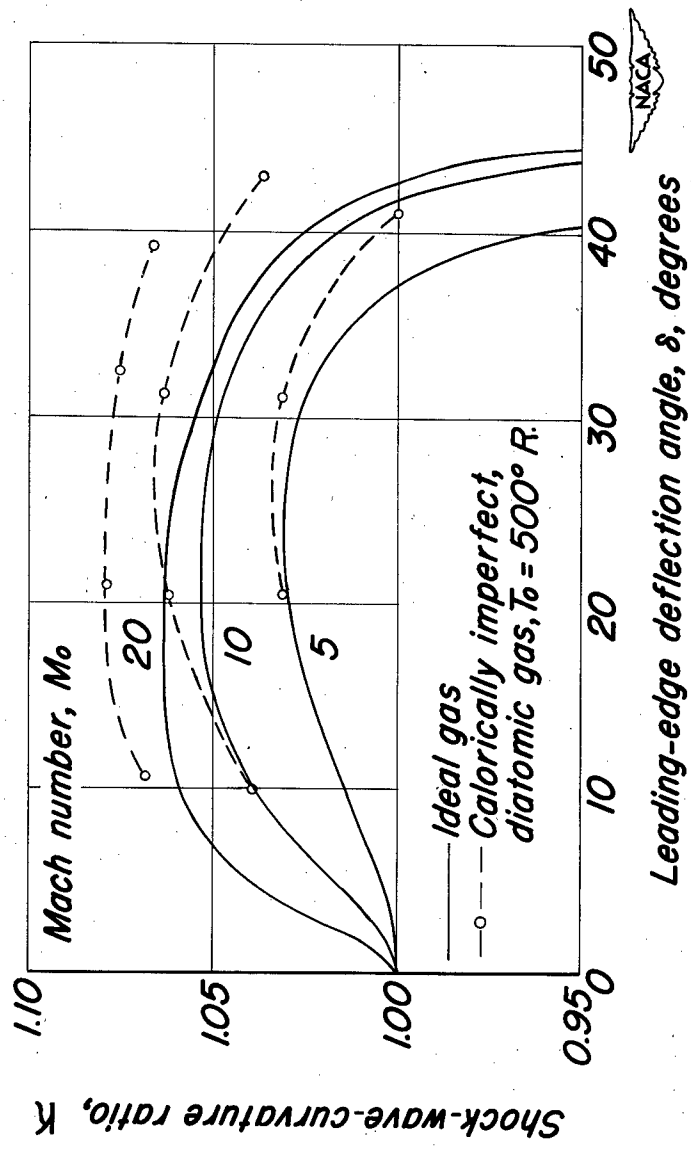

Figure 15.–Comparison of the variation of shock-wave-curvature ratio with leading-edge deflection angle for various free-stream Mach numbers for an ideal gas and for a calorically imperfect, diatomic gas.

NACA TN 2729
National Advisory Committee for Aeronautics.
AN ANALYSIS OF SUPERSONIC FLOW IN THE REGION OF THE LEADING EDGE OF CURVED AIRFOILS, INCLUDING CHARTS FOR DETERMINING SURFACE-PRESSURE GRADIENT AND SHOCK-WAVE CURVATURE. Samuel Kraus. June 1952. 45p. diagrs., 5 tabs. (NACA TN 2729)

Flow in the region of the leading edge of curved airfoils with attached shock waves is investigated. Tables and charts are presented for determining the surface-pressure gradient and shock-wave curvature in supersonic flow of an ideal diatomic gas. The results cover a range of Mach numbers from 1.5 to infinite and deflection angles from zero up to those approaching shock detachment. Calculations of surface-pressure gradient and shock-wave curvature are also made for curved airfoils in supersonic flow of a calorically imperfect, diatomic gas. An approximate procedure for determining the flow field a short dis-

Copies obtainable from NACA, Washington (over)

1. Flow, Supersonic (1.1.2.3)
2. Aerodynamics with Heat (1.1.4)
3. Wing Section Theory (1.2.1.1)
4. Mach Number Effects - Wing Sections (1.2.1.8)

I. Kraus, Samuel
II. NACA TN 2729

NACA TN 2729
National Advisory Committee for Aeronautics.
AN ANALYSIS OF SUPERSONIC FLOW IN THE REGION OF THE LEADING EDGE OF CURVED AIRFOILS, INCLUDING CHARTS FOR DETERMINING SURFACE-PRESSURE GRADIENT AND SHOCK-WAVE CURVATURE. Samuel Kraus. June 1952. 45p. diagrs., 5 tabs. (NACA TN 2729)

Flow in the region of the leading edge of curved airfoils with attached shock waves is investigated. Tables and charts are presented for determining the surface-pressure gradient and shock-wave curvature in supersonic flow of an ideal diatomic gas. The results cover a range of Mach numbers from 1.5 to infinite and deflection angles from zero up to those approaching shock detachment. Calculations of surface-pressure gradient and shock-wave curvature are also made for curved airfoils in supersonic flow of a calorically imperfect, diatomic gas. An approximate procedure for determining the flow field a short dis-

Copies obtainable from NACA, Washington (over)

1. Flow, Supersonic (1.1.2.3)
2. Aerodynamics with Heat (1.1.4)
3. Wing Section Theory (1.2.1.1)
4. Mach Number Effects - Wing Sections (1.2.1.8)

I. Kraus, Samuel
II. NACA TN 2729

NACA TN 2729
National Advisory Committee for Aeronautics.
AN ANALYSIS OF SUPERSONIC FLOW IN THE REGION OF THE LEADING EDGE OF CURVED AIRFOILS, INCLUDING CHARTS FOR DETERMINING SURFACE-PRESSURE GRADIENT AND SHOCK-WAVE CURVATURE. Samuel Kraus. June 1952. 45p. diagrs., 5 tabs. (NACA TN 2729)

Flow in the region of the leading edge of curved airfoils with attached shock waves is investigated. Tables and charts are presented for determining the surface-pressure gradient and shock-wave curvature in supersonic flow of an ideal diatomic gas. The results cover a range of Mach numbers from 1.5 to infinite and deflection angles from zero up to those approaching shock detachment. Calculations of surface-pressure gradient and shock-wave curvature are also made for curved airfoils in supersonic flow of a calorically imperfect, diatomic gas. An approximate procedure for determining the flow field a short dis-

Copies obtainable from NACA, Washington (over)

1. Flow, Supersonic (1.1.2.3)
2. Aerodynamics with Heat (1.1.4)
3. Wing Section Theory (1.2.1.1)
4. Mach Number Effects - Wing Sections (1.2.1.8)

I. Kraus, Samuel
II. NACA TN 2729

NACA TN 2729
National Advisory Committee for Aeronautics.
AN ANALYSIS OF SUPERSONIC FLOW IN THE REGION OF THE LEADING EDGE OF CURVED AIRFOILS, INCLUDING CHARTS FOR DETERMINING SURFACE-PRESSURE GRADIENT AND SHOCK-WAVE CURVATURE. Samuel Kraus. June 1952. 45p. diagrs., 5 tabs. (NACA TN 2729)

Flow in the region of the leading edge of curved airfoils with attached shock waves is investigated. Tables and charts are presented for determining the surface-pressure gradient and shock-wave curvature in supersonic flow of an ideal diatomic gas. The results cover a range of Mach numbers from 1.5 to infinite and deflection angles from zero up to those approaching shock detachment. Calculations of surface-pressure gradient and shock-wave curvature are also made for curved airfoils in supersonic flow of a calorically imperfect, diatomic gas. An approximate procedure for determining the flow field a short dis-

Copies obtainable from NACA, Washington (over)

1. Flow, Supersonic (1.1.2.3)
2. Aerodynamics with Heat (1.1.4)
3. Wing Section Theory (1.2.1.1)
4. Mach Number Effects - Wing Sections (1.2.1.8)

I. Kraus, Samuel
II. NACA TN 2729

NACA TN 2729

tance downstream of the leading edge is also presented.

Copies obtainable from NACA, Washington

NACA TN 2729

tance downstream of the leading edge is also presented.

Copies obtainable from NACA, Washington

NACA TN 2729

tance downstream of the leading edge is also presented.

Copies obtainable from NACA, Washington

NACA TN 2729

tance downstream of the leading edge is also presented.

Copies obtainable from NACA, Washington